NMR IN BIOMEDICINE
NMR Biomed. 2000;**13**:129–153

Proton NMR chemical shifts and coupling constants for brain metabolites

Varanavasi Govindaraju, Karl Young and Andrew A. Maudsley*

[1]Department of Radiology, University of California San Francisco and DVA Medical Center, 4150 Clement St (114M), San Francisco, CA 94121, USA

Received 5 November 1999; revised 29 December 1999; accepted 30 December 1999

ABSTRACT: Proton NMR chemical shift and *J*-coupling values are presented for 35 metabolites that can be detected by *in vivo* or *in vitro* NMR studies of mammalian brain. Measurements were obtained using high-field NMR spectra of metabolites in solution, under conditions typical for normal physiological temperature and pH. This information is presented with an accuracy that is suitable for computer simulation of metabolite spectra to be used as basis functions of a parametric spectral analysis procedure. This procedure is verified by the analysis of a rat brain extract spectrum, using the measured spectral parameters. In addition, the metabolite structures and example spectra are presented, and clinical applications and MR spectroscopic measurements of these metabolites are reviewed. Copyright © 2000 John Wiley & Sons, Ltd.

KEYWORDS: nuclear magnetic resonance spectroscopy; chemical shifts; coupling constants; proton; *in vivo*; brain metabolites; parametric spectral analysis; review

INTRODUCTION

Due to its relatively high sensitivity and ability to detect numerous tissue metabolites, proton NMR spectroscopy (MRS) has become well established as a non-invasive technique for studies of biological systems *in vivo* and *in vitro*. Quantitation of the NMR-observable metabolites can provide considerable biochemical information, and can help clinical investigators in understanding the role of metabolites in normal and pathological conditions. In recent years the biomedical and *in vivo* applications of ^{1}H spectroscopy have increased, in part due to the increased availability of high magnetic field strengths and improved spectrometer performance.

One difficulty associated with *in vivo* proton spectroscopy is the identification and measurement of individual metabolite contributions in spectra acquired at short *TE*. This is largely due to the presence of numerous unresolved multiplet groups exhibiting complex line shapes and considerable spectral overlap, which is particularly severe at the lower B_0 field strengths that are commonly available for studies in humans. Additional difficulties are caused by variable spectral patterns caused by susceptibility-induced line-shape distortions, the presence of broad uncharacterized resonances from macromolecules, lipids and unsuppressed water, and low signal-to-noise ratios. The analysis of data such as these is greatly facilitated by incorporating *a priori* spectral information in a parametric modeling approach.[1–5] For this purpose, considerable information on the chemical shifts of many observable metabolite resonances is available in several pioneering reports,[6–16] including a thorough review of resonance assignments by Arus *et al.*[8] Similar data has also been presented for analysis of plasma and cerebrospinal fluid.[17,18]

Chemical shift information alone is suitable for identification and quantitation of singlet resonances, observed at any field strength, or for situations where the data are always acquired under identical conditions to those used for the initial measurement of the individual metabolite resonances. For example, this limited information has been sufficient for *in vivo* measurement of creatine, choline and the acetyl moiety of *N*-acetylaspartate, all of which can be readily observed using long *TE* (e.g. $>$100 ms) measurements. For compounds having

**Correspondence to:* A. A. Maudsley, Magnetic Resonance Unit (114M), Veterans Affairs Medical Center, 4150 Clement Street, San Francisco, CA 94121, USA.
E-mail: maudsle@itsa.ucsf.edu
Contract/grant sponsor: PHS; *contract grant number:* AG12119.

Abbreviations used: Ace, acetate; Ala, alanine; Asp, aspartate; Cho, choline; Cr, creatine; DSS, 2,2-dimethyl-2-silapentane-5-sulfonate; GABA, γ-aminobutyric acid; Glc, D-glucose; Gln, glutamine; GSH, glutathione; Glu, glutamate; Gly, glycine; GPC, glycerophosphorylcholine; His, histidine; Lac, lactate; M-Ins, *myo*-inositol; NAA, *N*-acetylaspartate; NAAG, *N*-acetylaspartylglutamate; PC, phosphorylcholine; PCA, perchloric acid; PCr, phosphocreatine; PE, phosphorylethanolamine; Phe, phenylalanine; PKU, phenylketonuria; Ser, Serine; s-Ins, scyllo-inositol; Suc, succinate; Tau, taurine; Thr, threonine; Trp, tryptophan; Tyr, tyrosine; Val, valine.

multiple resonances, additional *a priori* information is available in terms of fixed frequency separations and relative amplitudes of the individual resonances belonging to each compound. However, unless some form of spectral-editing acquisition method is used to obtain a simplified spectrum, additional care is required for the analysis of compounds exhibiting multiplet resonances from spin-coupled nuclei. For these cases, identification using individual resonance frequencies is not only strongly field dependent, but also requires information on the phase of the individual resonances, which may be altered when using multiple-pulse spatial localization sequences. Additional experimental parameters may also alter the relative amplitudes between the resonances from the same compound. For this reason, previous reports describing automated spectral analysis methods that are based upon parametric modeling have obtained the *a priori* spectral information by using measurements of each of the known metabolites in solution.[1,2] To ensure that these reference spectra correspond with the spectral patterns seen in the sample under study, it is essential that they be measured using identical acquisition parameters as those used for the data to be analyzed, and for the same conditions of pH and temperature that exist in the sample, for example either *in vivo* or as used for the *in vitro* measurement.

An alternative approach for generating the *a priori* spectral information has been described by Young *et al.*,[4] where model spectra are generated for each metabolite by computer simulation to obtain a list of the relative frequencies, phases, and amplitudes of all resonances for each metabolite. This procedure requires information on the chemical shifts of each multiplet group, *J*-couplings, field strength, and the acquisition pulse sequence. This approach has advantages in that the required basis functions can be rapidly generated for any experimental conditions with great accuracy, and no sample preparation and additional spectrometer time are required. This method requires that the spectral parameters are known with a sufficient degree of accuracy and that the acquisition pulse sequence is correctly modeled, for example to account for the effects of selective pulse shapes[19] or chemical shift artifacts.[20] It is, of course, also necessary that the chemical shifts and coupling constants are known for all compounds that provide a significant contribution to the spectrum, although this is frequently unrealizable due to the presence of uncharacterized macromolecular and lipid resonances[21] that must be separately addressed in the analysis procedure.[22] The measurement of both chemical shift and coupling constants has been carried out for many metabolites, as for example, in the report of Behar *et al.*[13] However, the available information remains incomplete in terms of the number of NMR-visible metabolites, lack of uniformity in the measurement conditions, and the numerical precision to which the parameters have been reported. Our previous studies have indicated that in many cases, to obtain a simulated spectrum that agrees well with experimental data the chemical shift values are required to have a numerical precision of at least three decimal places.[4]

In this report, proton chemical shifts and coupling constants are presented for those metabolites that may be observed in human brain by *in vivo* or *in vitro* studies. Parameter values were determined from high-resolution NMR studies of individual metabolites in solution, performed for the same physiologically relevant conditions, and reported with a greater degree of precision than has previously been available in the literature. In a few cases, the measured values are supplemented by previously reported values, including our previously reported measurements for glutamate and glutamine.[23] The availability of this comprehensive list of spectral parameters makes possible the generation of model functions for parametric spectral analysis of proton spectra of brain, as has previously been demonstrated for *in vivo* ^{1}H spectroscopic imaging.[4,22] To verify the accuracy of these parameters, this procedure has been used in this report for analysis of an experimental spectrum from rat brain extract obtained at 600 MHz.

To provide a more complete review of the information that is potentially available using *in vivo* ^{1}H MRS, this report also includes a brief description of the known functions of each metabolite, the molecular structures, and an example of the individual metabolite spectra. While a thorough review of the field of *in vivo* proton MRS in brain is not provided, we have attempted to include references to significant NMR studies or biochemical texts where more detailed information may be found. Finally, a summary of metabolite concentration ranges in adult human brain, obtained from the existing literature, has been included for reference as well as to serve as an approximate guide to their relative spectral contributions and initial amplitude values for a parametric model. By providing NMR parameters, example spectra, and concentration ranges of brain metabolites, this report presents a starting point for implementation of a parametric spectral analysis of *in vivo* or *in vitro* proton spectra of brain, or optimization of pulse sequences using spectral simulation methods.[24]

The selection of compounds is limited to low molecular weight metabolites that are considered to be reasonably detectable in brain using conventional MRS techniques; i.e. that may be present with effective proton concentrations of approximately 0.5 mmol/kg of wet weight (kg_{ww}) or greater, either in normal brain or following increases with disease. Only the L-form amino acids are included. Measurement of NMR parameters is limited to conditions of normal brain pH and temperature, while identifying those molecular groups for which pH or temperature dependent changes may be expected over a physiologically relevant range, e.g. pH 6.5–7.5. Spectra were measured in solutions of both H_2O and D_2O, so as to also provide parameters relevant for extract studies in

D_2O, which requires accounting for the solvent isotope effect that results in small differences in chemical shift values. This effect is strongest for those metabolites containing exchangeable protons, resulting in measurable shifts even over several bond lengths away from the exchange site. The International Union of Pure and Applied Chemistry (IUPAC) nomenclature* has been used for numbering the molecular groups.[25]

METHODS

Solutions of the 35 metabolites (from Sigma Chemical Co., St Louis, MO, USA) shown in Fig. 1 were prepared at 100 mM [lower concentrations of 3–5 mM were used for tryptophan tyrosine, *N*-acetylaspartylglutamate (NAAG), and homocarnosine] both in D_2O at 6.6 pH (meter reading, glass isotope effect[26]) and in H_2O at pH 7.0. The solution pH was adjusted using solutions of NaOH and HCl. A small amount of sodium salt of 2,2-dimethyl-2-silapentane-5-sulfonate (DSS) was added to the solutions as a chemical shift reference.[27] All chemical shifts are reported with reference to the trimethyl hydrogen resonance of DSS set at 0.0 ppm. Proton NMR spectra were acquired using a pulse-acquire sequence at either 500 or 600 MHz proton frequency and data collected at 37 °C. Typical parameters used for the data acquisition were: sweep width = 6 kHz, data size = 32K points, TR = 20 s, and 32 FID averages. Spectra were zero-filled to 64K points before Fourier transformation. In addition, two dimensional ECOSY data were obtained for NAAG at 500 MHz and glutathione at 600 MHz. These studies used a spectral width of 2732 Hz, 1024 steps in f1-dimension, and a repetition delay of 7.8 s. Heteronuclear (^{31}P and ^{14}N) decoupling and ^{1}H observe, and heteronuclear observe experiments were also carried out for cholines and ethanolamines at 500 MHz proton frequency spectrometer.

Chemical shifts and *J*-coupling constants were first estimated by direct measurement from the spectra, then these values, together with initial guess values for the remaining shifts and coupling constants, were submitted to a spectral simulation and optimization program (NUTS, Acorn NMR, California, USA). Negative *J*-coupling values for geminal couplings and positive *J*-coupling values for vicinal couplings were given. The output of the optimization program gave a complete set of optimized values by comparing experimental spectra with simulated spectra. This automatic optimization procedure assumes Lorentzian lineshapes and uses the Simplex algorithm to optimize chemical shifts, coupling constants, amplitude and linewidth by minimizing the squared difference between the calculated and the experimental spectra. For compounds containing choline and ethanolamine moieties, a spectral simulation and optimization program was developed in house, which allowed couplings with nitrogen and phosphorus to be correctly accounted for. This program used a nonlinear least squares minimization procedure to optimize spectral parameters, using a simulation of the spectrum generated with the GAMMA[28] NMR library.

To estimate the measurement error, the acquisition of a spectrum for *myo*-inositol was repeated 12 times, carried out over two sessions, and starting with miss-set shim values and automatic shimming performed before each acquisition. The standard deviations of the resultant chemical shift and *J*-coupling values were then calculated.

Using the measured chemical shift and *J*-coupling values, spectra were simulated for N-acetylaspartate (NAA) and *myo*-inositol using programs based on the GAMMA library[4,28] and assuming the same FID acquisition and field strength as the initial high-resolution spectroscopic measurement. These results were then compared with the acquired data. Additional spectra were acquired for these same metabolite solutions at a field strength of 1.5 T, using PRESS and STEAM acquisitions, at several *TE* values ranging from 25 to 270 ms, and these data were again compared with simulation results obtained for this field strength. Additionally, spectra for all metabolites were generated for 4.0 T, using a relatively narrow line width in comparison to that observed *in vivo*, in order to illustrate their spectral patterns. This field strength was chosen to provide a simpler spectrum, in light of strong coupling effects at lower fields and increased chemical shift dispersion at higher fields. Furthermore, this field strength is becoming increasingly available for spectroscopic studies in humans.

Perchloric acid (PCA) extract of a Wistar rat brain (male, 260 g weight) was prepared in D_2O at pH 6.6 (meter reading) by homogenizing 2.1 g of cerebral tissue with 12% PCA as described elsewhere.[29] For 600 MHz NMR spectral recording, 300 µl of the extract together with a small amount of DSS as a chemical shift reference was taken in a 5 mm dia. NMR tube. A spectrum was obtained at 37 °C, using a water-presaturation pulse-acquire sequence with a sweep-width of 6 kHz, 32K data points, TR = 20 s, and 64 averages. The resultant spectrum was then analyzed using an automated parametric spectral analysis procedure previously described.[4,5] For this purpose, a spectral database containing the frequencies, relative amplitudes and phase of all resonances, for all metabolites, was generated by computer simulation using the previously determined metabolite parameters measured in D_2O. Also included in this model were resonances of DSS at 0.0 and 2.90 ppm. This information then provided the *a priori* information

*For some metabolites the IUPAC numbering of molecular groups may differ from that commonly used by biochemists, for example with the imidazole ring of histidine and histamine.

Acetate

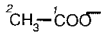

N-acetylaspartate

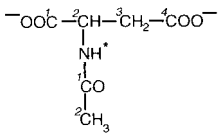

N-acetylaspartylglutamate

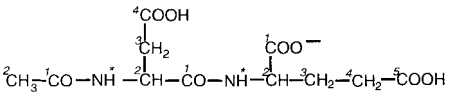

Adenosine Triphosphate

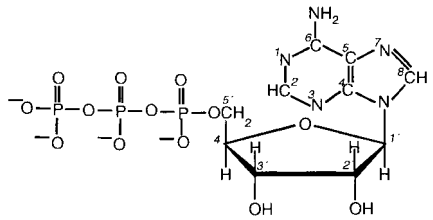

Alanine

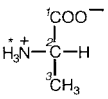

Gamma aminobutyric acid

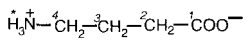

Aspartate

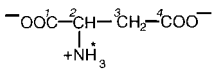

Choline

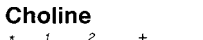

Creatine

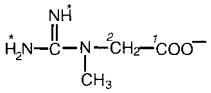

Ethanolamine

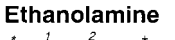

Glucose

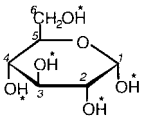

Glutamate

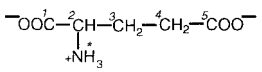

Glutamine

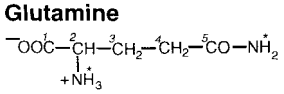

Glutathione

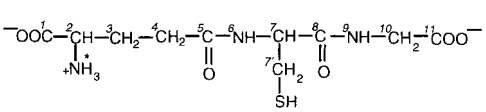

Glycerol

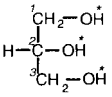

Glycerophosphorylcholine

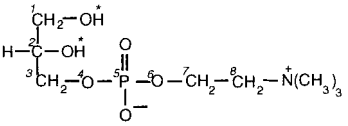

Glycine

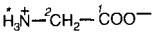

Histamine

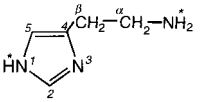

Histidine

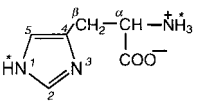

Homocarnosine

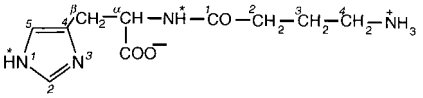

***myo*-Inositol**

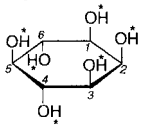

***scyllo*-Inositol**

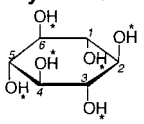

Lactate

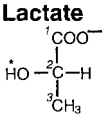

Phenylalanine

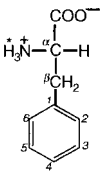

Phosphocreatine

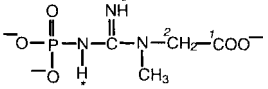

Phosphorylcholine

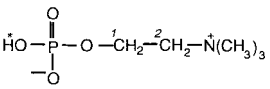

Phosphorylethanolamine

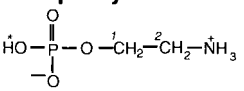

Pyruvate

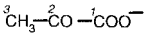

Serine

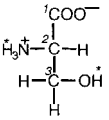

Succinate

Taurine

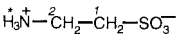

Threonine

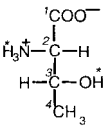

Tryptophan

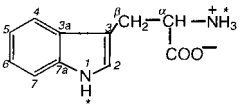

Tyrosine

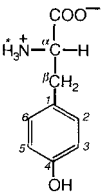

Valine

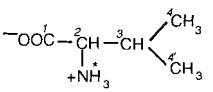

Figure 1. Chemical structures for several metabolites observable by ^{1}H NMR in mammalian brain. Exchangeable protons are indicated by the asterisks and assignments of the molecular groups follow the IUPAC nomenclature

Table 1. Proton chemical shift and *J*-coupling values for low molecular weight brain metabolites. Chemical shifts are reported with reference to DSS-trimethyl singlet resonance at 0.0000 ppm, and multiplicity definitions are: s, singlet; d, doublet; t, triplet; q, quartet; qu, quintet; m, other multiplet. The multiplicity given here was observed in conventional one-dimensional spectra recorded at 500 or 600 MHz. Multiplet groups having a pH-dependent chemical shift in the physiological range are indicated by an asterisk

Compound	Group	Shift (ppm) in H_2O	Shift (ppm) in D_2O	Multiplicity	*J* (Hz)	Connectivity
Acetate	$^{2}CH_3$*	1.9040	1.9030	s	None	
NAA						
Acetyl moiety	$^{2}CH_3$	2.0080	2.0050	s		
Aspartate moiety	^{2}CH	4.3817	4.3823	dd	3.861	2–3
	$^{3}CH_2$	2.6727	2.6759	dd	9.821	2–3′
		2.4863	2.4866	dd	−15.592	3–3′
	NH	7.8205	7.8155	d	6.400	NH-2
NAAG[a]						
Acetyl moiety	$^{2}CH_3$		2.042	s	None	
Aspartyl moiety	^{2}CH		4.607	dd	4.412	2–3
	$^{3}CH_2$		2.721	dd	9.515	2–3′
			2.519	dd	−15.910	3–3′
Glutamate moiety	^{2}CH		4.128	dd		
	$^{3}CH_2$		1.881	m		
			2.049	m		
	$^{4}CH_2$		2.190	m		
			2.180			
ATP[b]						
Ribose moiety	$^{1'}CH$	6.126†	6.129	d	5.7	1′–2′
	$^{2'}CH$		4.796	t	5.3	2′–3′
	$^{3'}CH$		4.616	dd	3.8	3′–4′
	$^{4'}CH$		4.396	qu	3.0	4′–5′
	$^{5',5''}CH_2$		4.295	m	3.1	4′–5″
			4.206	m	−11.8	5′–5″
					1.9	4′-P
					6.5	5′-P
					4.9	5″-P
Adenosine moiety	^{2}CH	8.224†	8.234	s		
	^{8}CH	8.514†	8.522	s		
	NH_2	6.755†		s		
Alanine	^{2}CH	3.7746	3.7680	q	7.234	2–3
	$^{3}CH_3$	1.4667	1.4655	d	−14.366	3–3′, 3″
					−14.366	3′–3″
GABA	$^{2}CH_2$	3.0128	3.0082	m	5.372	2–3
					7.127	2–3′
	$^{3}CH_2$	1.8890	1.8888	qu	10.578	2′–3
					6.982	2′–3′
	$^{4}CH_2$	2.2840	2.2828	t	7.755	3–4
					7.432	3–4′
					6.173	3′–4
					7.933	3′–4′
Aspartate	^{2}CH	3.8914	3.8867	dd	3.647	2–3
	$^{3}CH_2$	2.8011	2.8021	dd	9.107	2–3′
		2.6533	2.6508	dd	−17.426	3–3′
Choline	$N(CH_3)_3$	3.1850	3.1890	s	None	
	$^{1}CH_2$	4.0540	4.0500	m	3.140	1–2
	$^{2}CH_2$	3.5010	3.5060	m	6.979	1–2′
					3.168	1′–2′
					7.011	1′–2
					2.572	1-N
					2.681	1′-N
					0.57	$N\text{-}CH_3$
Creatine	$N(CH_3)$	3.0270	3.0260	s	None	
	$^{2}CH_2$	3.9130	3.9110	s	None	
	NH	6.6490		s	None	
Ethanolamine	$^{1}CH_2$	3.8184		m	3.897	1–2
	$^{2}CH_2$	3.1467		m	6.794	1–2′
					6.694	1′–2

Table 1. ***Continued.***

Compound	Group	Shift (ppm) in H_2O	Shift (ppm) in D_2O	Multiplicity	*J* (Hz)	Connectivity
Ethanolamine (cont.)					3.798	1′–2′
					0.657	1-N
					0.142	1′-N
D-Glucose[c]						
α-anomer	^{1}CH		5.216	d	3.8	1–2
	^{2}CH		3.519	dd	9.6	2–3
	^{3}CH		3.698	t	9.4	3–4
	^{4}CH		3.395	t	9.9	4–5
	^{5}CH		3.822	m	1.5	5–6
	^{6}CH		3.826	dd	6.0	5–6′
	$^{6'}$CH		3.749	dd	−12.1	6–6′
β-anomer	^{1}CH		4.630	d	8.0	1–2
	^{2}CH		3.230	dd	9.1	2–3
	^{3}CH		3.473	t	9.4	3–4
	^{4}CH		3.387	t	8.9	4–5
	^{5}CH		3.450	m	1.6	5–6
	^{6}CH		3.882	dd	5.4	5–6′
	$^{6'}$CH		3.707	dd	−12.3	6–6′
Glutamate	^{2}CH	3.7433	3.7444	dd	7.331	2–3
	$^{3}CH_2$	2.0375	2.0424	m	4.651	2–3′
		2.1200	2.1206		−14.849	3–3′
	$^{4}CH_2$	2.3378	2.3354	m	8.406	3–4′
		2.3520	2.3507		6.875	3′–4′
					6.413	3–4
					8.478	3′–4
					−15.915	4–4′
Glutamine	^{2}CH	3.7530	3.7625	t	5.847	2–3
	$^{3}CH_2$	2.1290	2.1360	m	6.500	2–3′
		2.1090	2.1180		−14.504	3–3′
	$^{4}CH_2$	2.4320	2.4350	m	9.165	3–4
		2.4540	2.4570		6.347	3–4′
					6.324	3′–4
					9.209	3′–4′
					−15.371	4–4′
	NH_2	6.8160		s		
		7.5290		s		
Glutathione[d]						
Glycine moiety	$^{10}CH_2$	3.769		s		
	^{9}NH	7.154		t		
Cysteine moiety	^{7}CH	4.5608		dd	7.09	7–7′
	$^{7'}CH_2$	2.9264		dd	4.71	7–7″
		2.9747		dd	−14.06	7′–7″
	^{6}NH	8.1770		d		
Glutamate moiety	^{2}CH	3.769		t	6.34	2–3
	$^{3}CH_2$	2.159		m	6.36	2–3′
		2.146		m	−15.48	3–3′
	$^{4}CH_2$	2.510		m	6.7	3–4
		2.560		m	7.6	3–4′
					7.6	3′–4
					6.7	3′–4′
					−15.92	4–4′
Glycerol	$^{1}CH_2$	3.5522	3.5486	dd	−11.715	1–1′, 3–3′
		3.6402	3.6364	dd	4.427	1–2, 2–3
	^{2}CH	3.7704	3.7680	m	6.485	1′–2, 2–3′
	$^{3}CH_2$	3.5522	3.5486	dd		
		3.6402	3.6363	dd		
Glycero-phosphocholine[a]						
Glycerol moiety	$^{1}CH_2$	3.605		dd	5.77	1–2, 2–3
		3.672		dd	4.53	1′–2, 2–3′
	^{2}CH	3.903		m		
	$^{3}CH_2$	3.871		m		
		3.946		m		
Choline moiety	$^{7}CH_2$	4.312		m	3.10	7–8, 7′–8′

Table 1. ***Continued.***

Compound	Group	Shift (ppm) in H_2O	Shift (ppm) in D_2O	Multiplicity	*J* (Hz)	Connectivity
Choline moiety (cont.)					2.67	7,7′-N
	$^{8}CH_2$	3.659		m	5.90	7–8′, 7′–8
	$N(CH_3)_3$	3.212		s	6.03	3,3′-P; 7,7′-P
Glycine	$^{2}CH_2$	3.5480	3.5450	s	None	
Histamine	$^{\alpha}CH_2$	2.9813	3.0320	m	−16.120	α–α′
		2.9897	3.0420		6.270	α′–β′
	$^{\beta}CH^2$	3.2916	3.3148	t	8.147	α–β′
					7.001	α′–β
					6.868	α–β
					−14.145	β–β′
Imidazole ring	^{2}CH*	7.8520	8.0250	d	1.07	2-^{1}NH
	^{5}CH*	7.0940	7.1620	m	1.19	5-^{1}NH
					0.73	5-β,β′
Histidine	$^{\alpha}CH$	3.9752	3.9959	dd	7.959	α–β
	$^{\beta}CH_2$	3.1195	3.1866	dd	4.812	α–β′
		3.2212	3.2644	dd	−15.513	β–β′
Imidazole ring	^{2}CH*	7.7910	7.9010	d	1.07	2-^{1}NH
	^{5}CH*	7.0580	7.1030	m	1.20	5-^{1}NH
					0.72	5-β,β′
Homocarnosine[a]	$^{\alpha}CH$	4.472		m	6.88	α-NH
	$^{\beta}CH_2$	3.185		dd		
		3.003		dd		
Imidazole ring	^{2}CH*	7.075		s		
	^{5}CH*	8.081		d		
GABA moiety	$^{2}CH_2$	2.962		m		
	$^{3}CH_2$	1.891		m		
	$^{4}CH_2$	2.367		m		
		7.899		d		
	NH_3	6.397		s		
Myo-inositol	^{1}CH	3.5217	3.5177	dd	2.889	1–2
	^{2}CH	4.0538	4.0488	t	9.998	1–6
	^{3}CH	3.5217	3.5177	dd	3.006	2–3
	^{4}CH	3.6144	3.6114	t	9.997	3–4
	^{5}CH	3.2690	3.2652	t	9.485	4–5
	^{6}CH	3.6144	3.6114	t	9.482	5–6
Scyllo-inositol	^{1-6}CH	3.3400	3.3340	s	None	
Lactate	^{2}CH	4.0974	4.0908	q	6.933	2–3
	$^{3}CH_3$	1.3142	1.3125	d		
Phenylalanine	$^{\alpha}CH$	3.9753	3.9829	dd	5.209	α–β
	$^{\beta}CH_2$	3.2734	3.2827	dd	8.013	α–β′
		3.1049	3.1132	dd	−14.573	β–β′
Phenyl ring	^{2}CH	7.3223	7.3223	m	7.909	2–3
	^{3}CH	7.4201	7.4201	m	1.592	2–4
	^{4}CH	7.3693	7.3693	m	7.204	3–4
	^{5}CH	7.4201	7.4201	m	0.493	2–5
	^{6}CH	7.3223	7.3223	m	0.994	3–5
					7.534	4–5
					1.419	2–6
					0.462	3–6
					0.970	4–6
					7.350	5–6
Phosphocreatine	$N(CH_3)$	3.0290	3.0280	s	None	
	$^{2}CH_2$	3.9300	3.9260	s	None	
	NH	6.5810[e]		s	None	
	NH	7.2960[e]		s	None	
Phosphoryl choline	$^{1}CH_2$	4.2805	4.2851	m	2.284	1–2
					7.231	1–2′
					2.235	1′–2′
					7.326	1′–2
	$^{2}CH_2$	3.6410	3.6440	m	2.680	1-N
					2.772	1′-N
					6.298	1-P

Table 1. ***Continued.***

Compound	Group	Shift (ppm) in H_2O	Shift (ppm) in D_2O	Multiplicity	*J* (Hz)	Connectivity
Phosphoryl choline (cont.)	$N(CH_3)$	3.2080	3.2100	s	6.249	1′-P
Phosphoryl ethanolamine	$^{1}CH_2$	3.9765	3.9825	m	3.182	1–2
					7.204	1′–2
					6.716	1–2′
					2.980	1–2′
	$^{2}CH_2$	3.2160	3.2150	m	7.288	1-P
					7.088	1′-P
					0.464	1-N
					0.588	1′-N
Pyruvate	$^{3}CH_3$	2.3590	2.3550	s	None	
Serine	^{2}CH	3.8347	3.8349	dd	5.979	2–3
	$^{3}CH_2$	3.9379	3.9352	dd	3.561	2–3′
		3.9764	3.9764	dd	−12.254	3–3′
Succinate	$^{2}CH_2$	2.3920	2.3970	s	None	
	$^{3}CH_2$	2.3920	2.3970	s	None	
Taurine	$^{1}CH_2$	3.4206	3.4190	t	6.742	1–2
					6.403	1′–2
	$^{2}CH_2$	3.2459	3.2473	t	6.464	1–2′
					6.792	1–2′
Threonine	^{2}CH	3.5785	3.5784	d	4.917	2–3
	^{3}CH	4.2464	4.2444	m	6.350	3–4
	$^{4}CH_3$	1.3158	1.3169	d		
Tryptophan	$^{\alpha}CH$	4.0468	4.0483	dd	4.851	α–β
	$^{\beta}CH_2$	3.4739	3.4787	dd	8.145	α–β′
		3.2892	3.2949	dd	−15.368	β–β′
Indole ring	^{2}CH	7.3120	7.3112	s	None	
	^{4}CH	7.7260	7.7255	d	7.600	4–5
	^{5}CH	7.2788	7.2759	t	1.000	4–6
	^{6}CH	7.1970	7.1934	t	7.507	5–6
	^{7}CH	7.5360	7.5315	d	0.945	4–7
					1.200	5–7
					7.677	6–7
Tyrosine	$^{\alpha}CH$	3.9281	3.9299	dd	5.147	α–β
	$^{\beta}CH_2$	3.1908	3.1965	dd	7.877	α–β′
		3.0370	3.0434	dd	−14.726	β–β′
Phenyl ring	^{2}CH	7.1852	7.1880	m	7.981	2–3
	^{3}CH	6.8895	6.8916	m	0.311	2–5
	^{5}CH	6.8895	6.8916	m	2.445	3–5
	^{6}CH	7.1852	7.1880	m	2.538	2–6
					0.460	3–6
					8.649	5–6
Valine	^{2}CH	3.5953	3.5954	d	4.405	2–3
	^{3}CH	2.2577	2.2622	m	6.971	3–4
	$^{4}CH_3$	1.0271	1.0290	d	7.071	3–4′
	$^{4'}CH_3$	0.9764	0.9793	d		

[a]Chemical shifts and coupling constants for these compounds were measured from the conventional one- and two-dimensional E.COSY (for NAAG only) spectra, and the values were not optimized.
[b]From Son and Chachaty [64]; data acquired at 35°C, the solution pH was neutral (between 7 and 8) and the chemical shift reference used was DSS. Multiplicity given here was observed at 250 MHz. †This list also includes values obtained from our measurements, for data acquired at 600 MHz.
[c]From Perkins *et al*[94]; data acquired at 25 °C and the sample pH not known. Multiplicity given here was observed at 270 MHz.
[d]Coupling constants for glutathione were measured from its two-dimensional ECOSY spectra acquired at 500 MHz, and were optimized only for the cystine moiety.
[e]These two NH resonances are from —C═NH— and —NH—P— protons; however, no specific assignments have been made.

used to generate the parametric spectral model. The fit procedure allowed for a mixed Lorentzian–Gaussian lineshape that was common to all resonances, and a non-parametric baseline characterization that accounted for any broad signal components.[22]

RESULTS AND DISCUSSION

The chemical shifts and coupling constants determined for each metabolite are presented in Table 1. Chemical shift values are given relative to DSS at 0.0 ppm, for pH

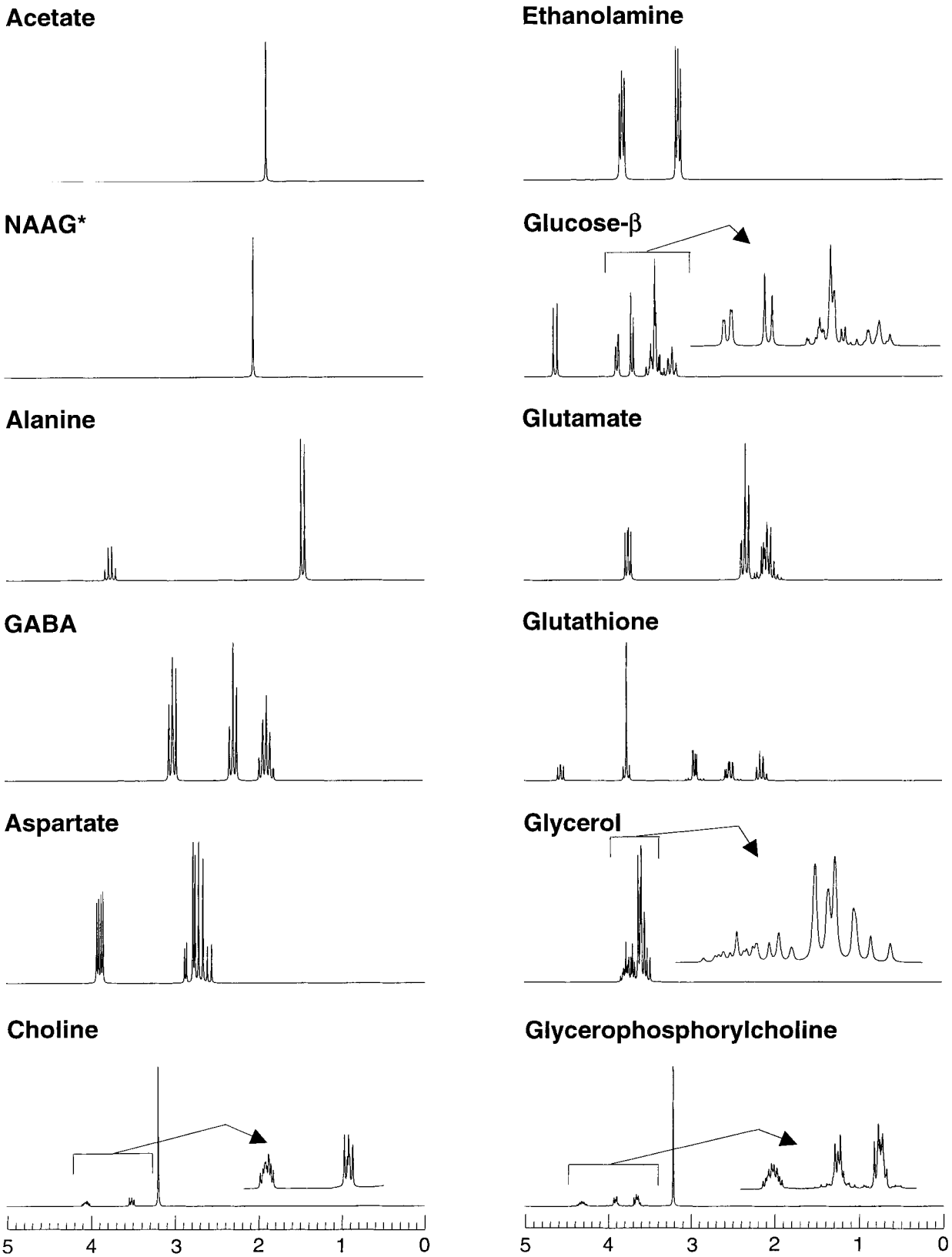

Figure 2. Spectral patterns for each metabolite at a field strength of 4.0 T with a line width of 1 Hz, simulated for FID observation using the experimentally measured NMR parameters shown in Table 1. Spectra are grouped for different ppm ranges of 0–5 ppm and 0–10 ppm. Also shown is the spectrum for DSS over the range of 0–3.5 ppm. The asterisks indicate that, for NAAG and homocarnosine, only the singlet downfield resonances were included in the simulation. The spectrum for succinate was not included as its only singlet resonance appears approximately at the pyruvate singlet resonance

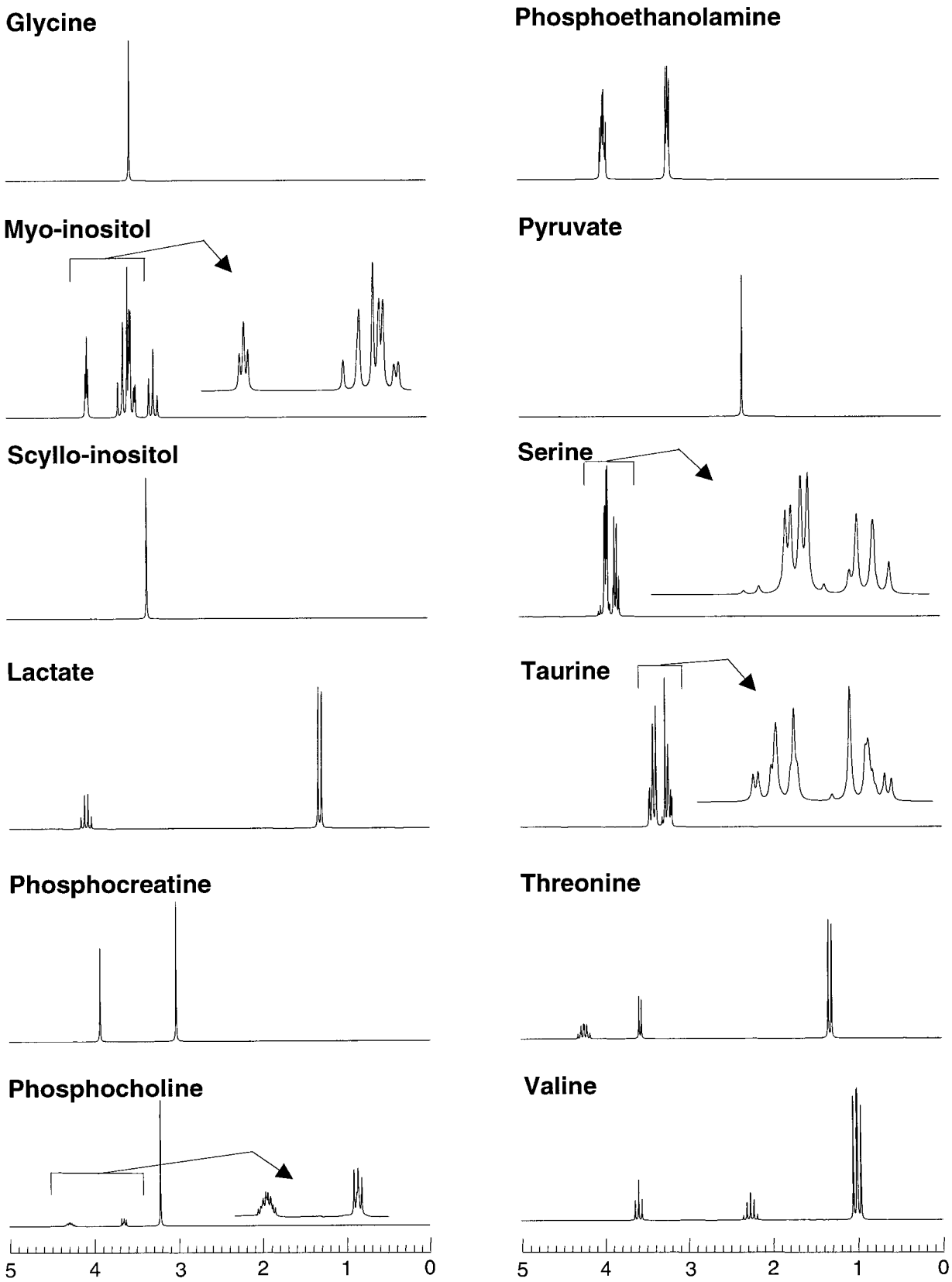

Figure 2. Continued.

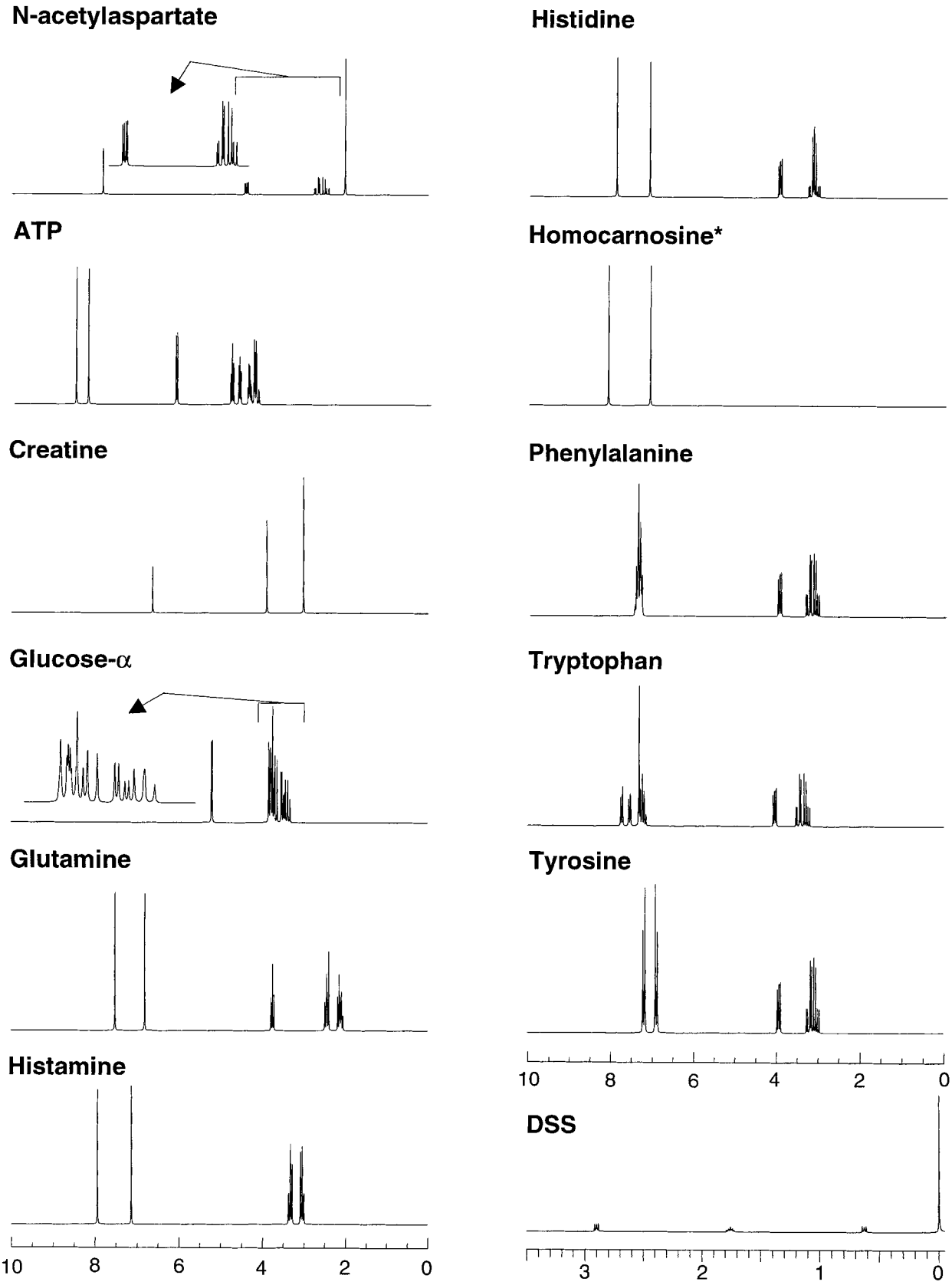

Figure 2. Continued.

Table 2. Ranges of MR-observable metabolite concentrations reported for normal adult human brain and biopsy tissues obtained using a variety of analytical techniques including *in vivo* MRS. Values have been rounded to one decimal place

Metabolite	Concentration range ($mmol/kg_{ww}$)	References
Acetate	0.4–0.8	31
NAA	7.9–16.6 (average 10.3)	50,72
NAAG	0.6–2.7	59
ATP	3.0	63
Alanine	0.2–1.4	72,161,162
GABA	1.3–1.9	72,161
Aspartate	1.0–1.4	72,162
Choline (total)	0.9–2.5	50,161
Creatine	5.1–10.6	50,72,161
Ethanolamine	3.3[a]	16
Glucose	1.0	90
Glutamate	6.0–12.5	72,76,161,162
Glutamine	3.0–5.8	14,72,162
Glutathione	2.0	162
Glycerol	<0.1	
Glycerophosphorylcholine	1.0	74
Glycine	0.4–1.0	161,162
Histamine	<0.1[a]	118
Histidine	0.09	162
Homocarnosine	0.23	162
Myo-inositol	3.8–8.1	50,72,161
Scyllo-inositol	0.3–0.6	137
Lactate	0.4	161
Phenylalanine	<0.1	162
Phosphocreatine	3.2–5.5	63,77
Phosphorylcholine	0.6	74
Phosphorylethanolamine	1.1–1.5	74,77,162
Pyruvate	0.2	31
Serine	0.4	162
Succinate	0.4	31
Taurine	0.9–1.5	72,161,162
Threonine	0.3	162
Tryptophan	<0.1	163
Tyrosine	<0.1	162
Valine	0.1	162

[a]From normal rodent brain.

of 7.0 and a temperature of 37 °C. The multiplicities indicated for each group correspond to the weak-coupling regime, and known pH dependencies in the physiological range are indicated by an asterisk. This table does not include resonances from protons that are in rapid exchange with water, or are present with very short T_2. From the repeated measurement of *myo*-inositol, we estimate a standard deviation for the measured chemical shifts of ± 0.0004 ppm, and for the *J*-coupling values of ± 0.004 Hz. For some of the compounds, as indicated in the text, the complete spectral optimization could not be carried out and these parameters are reported with a corresponding reduction in accuracy in Table 1.

Excellent agreement between the spectra obtained experimentally in solution at 1.5 T and the spectra simulated using the determined metabolite parameters was found (data not shown), including accounting for the effects of *J*-modulation, similar to previously demonstrated results.[4] Example spectra for each metabolite are presented in Fig. 2, which have been simulated for a field strength of 4.0 T and a FID observation. In Table 2 are shown a range of the reported concentrations of each metabolite in normal adult human brain, obtained from published literature values.

In the following section, we provide further discussion on each metabolite.

Acetate (Ace)

Acetate is an essential building block for synthesis of a number of compounds. Its presence has been reported in several cell culture and extract studies, though its abundance was questioned as a possible artifact of the sample preparation.[11] Nevertheless, it has been observed in high-resolution NMR studies of normal rat brain,[30] human resected tissues,[31] and cell cultures,[32] and to be present at a high concentration in neonatal rat cerebellum with a progressive decrease with age.[33] Concentrations in human brain are approximately 0.4–0.8 $mmol/kg_{ww}$,[31] with increased levels observed in brain tumors,[34] ischemia,[35] and *in vivo* in brain abscesses.[36] In extracts, decreased acetate has been found to correlate with changes of NAA with multiple sclerosis.[37] Acetate is a simple molecule containing a single CH_3 group that provides a singlet at 1.90 ppm, which is shifted downfield at lower pH.[38]

N-Acetyl aspartate (NAA)

NAA is a free amino acid present in the brain at relatively high concentrations (second only to glutamic acid in total free amino acid concentration). It is localized primarily in the central and peripheral nervous system,[39,40] although it has also been reported to be present in the eye.[41] Its function is poorly understood, but it is believed to act as an osmolite, a storage form of aspartate, a precursor of NAAG, as well as having a variety of other functions.[39,42] It is broken down into aspartate and acetate by the enzyme asparto-acylase.

The abundance of NAA and the presence of a prominent singlet resonance greatly facilitate MR observation *in vivo*, and it has been widely studied for many clinical neurological and neuropsychiatric applications.[39,42,43] Brain NAA is commonly believed to provide a marker of neuronal density, although this is not fully substantiated as NAA concentrations differ among neuron types;[44] it has also been found in other cell types;[45] and dynamic changes of neuronal concentrations have been observed, indicating that NAA levels may also reflect neuronal dysfunction rather than loss. For

example, recovery of NAA levels has been observed with incomplete reversible ischemia[46] and brain injury,[47] and reduced NAA levels have also been observed with multiple sclerosis in the absence of neuronal loss.[42] Increased NAA levels have also been observed with Canavan disease.[42,48]

NAA has seven protons that give NMR signals between 2.0 and 8.0 ppm. It typically provides the most prominent resonance, a singlet at 2.01 ppm, from the three protons of an *N*-acetyl CH_3 group. In one-dimensional *in vivo* spectra at lower field strengths, this resonance may also contain smaller contributions from NAAG, though this can be separated at higher field strengths or by using two-dimensional methods.[46] NAA also has three doublet-of-doublets centered at 2.49, 2.67 and 4.38 ppm that correspond to the protons of aspartate CH_2 and CH groups. These three protons form an ABX spin system with eight resonance lines for the CH_2 group and four resonance lines for the CH group. The amide NH proton, which is exchangeable with water-protons, gives a broad doublet at 7.82 ppm that is known to be temperature dependent.[49]

The typical concentration and *in vivo* relaxation rates of the cerebral *N*-acetyl containing metabolites in humans have been reported in several studies (reviewed by Kreis,[50] see also Pouwels and Frahm[51] and Wang and Li[52]). Reported concentrations in human brain are in the range of 7–16 mmol/kg_{ww}. Decreased NAA concentrations in cortical gray matter have been reported with age,[53] although no correlations were observed in another report.[54]

N-Acetylaspartylglutamate (NAAG)

N-acetylaspartylglutamate is a dipeptide of *N*-substituted aspartate and glutamate. It is present in the central and peripheral nervous systems of several species, and reported to be unevenly distributed within the brain with a concentration range of 0.6–3 mM[40,55–59] that is known to be regionally altered in neuropsychiatric disorders.[60,61] NAAG is suggested to be involved in excitatory neurotransmission as well as a source of glutamate,[60] although its function remains to be clearly established.

Holowenko *et al.*[62] first reported a high-resolution ^{1}H NMR study of NAAG in perchloric acid extracts of rat nervous tissues, and Pouwels and Frahm[59] have reported the distribution of NAAG in different regions of human brain. The NAAG molecule consists of acetyl, aspartyl and glutamate moieties, with 11 non-exchangeable protons and three water-exchangeable protons. Since NAAG is structurally similar to NAA and glutamate many of their resonance multiplets overlap. For *in vivo* studies at lower field strengths, it is primarily detected via the acetyl-CH_3 protons that give a singlet resonance at 2.04 ppm, and which therefore appears as a shoulder of the NAA CH_3 resonance. The chemical shifts and the coupling constants reported in Table 1 were not optimized to obtain greater accuracy beyond that obtained from the two-dimensional E-COSY measurement. This was due to difficulties associated with the overlap of the singlet from the acetyl-CH_3 protons with the multiplet from the glutamate ^{3}CH moiety centered at 2.05 ppm, which prevented convergence of the optimization procedure. Additionally, a singlet from CH_3 protons from acetate impurity overlapped with the multiplet from the glutamate ^{3}CH proton multiplet centered at 1.88 ppm.

Adenosine triphosphate (ATP)

Together with phosphocreatine (PCr), adenosine triphosphate is the principal donor of free energy in biological systems. It is a nucleotide, a high-energy phosphate compound, which consists of adenine, ribose and triphosphate units. Its normal concentration in the human brain is 3 mmol/kg_{ww}.[63]

The analysis of coupling patterns for ATP is complex, and since its signal contributions upfield from water are small, our measurements are limited to only the downfield region where *in vivo* ^{1}H MRS detection is possible.[14] The chemical shifts and coupling constants presented in Table 1 represent a combination of our measurements for the downfield region, and those from the report of Son and Chachaty,[64] which were for an ATP solution in D_2O at 7–8 pH and acquired at 250 MHz. However, differences between these previously reported literature values[64] and ours were noted, typically in the second decimal place, which are probably due to slightly different experimental conditions of temperature and pH. In the ATP adenine-ring, the ^{2}CH and ^{8}CH protons resonate as singlets at 8.22 and 8.51 ppm, respectively. These ring-CH protons exchange slowly with water, and although two separate peaks are seen in solution, only one peak is observed at 8.22 ppm *in vivo*.[14] These resonances are also pH dependent. The NH_2 protons give a broad line at 6.75 ppm and the ribose-$^{1'}$CH proton gives a doublet centered at 6.13 ppm. The remaining resonances occur in several multiplets in the range of 4.2–4.8 ppm.

Alanine (Ala)

Alanine, a nonessential amino acid that contains a methyl group, and is present in the human brain at approximately 0.5 mmol/kg_{ww}. Increased alanine has been observed *in vivo* in meningiomas[65] and following ischemia.[16,46,66] The $^3CH_3$ and ^{2}CH protons of alanine form a weakly coupled AX_3 system, similar to lactate, with a doublet at 1.47 ppm and a quartet at 3.77 ppm. Its chemical shifts exhibit pH dependence, though outside of the physiolo-

gical range. To improve *in vivo* observation where spectral overlap with lipid resonances may obscure measurement, the doublet may be observed using selective irradiation editing techniques[67] or observation at longer *TE*s, as are similarly used for lactate.

γ-Aminobutyric acid (GABA)

GABA is a primary inhibitory neurotransmitter that is present in the brain at a concentration of approximately 1 mmol/kg_{ww}, although altered concentrations are associated with several neurological disorders. Increased GABA levels in the brain have been used for treatment of epileptic seizures and muscle spasms, and ^{1}H MRS observation has been proposed to monitor its concentration in the brain.[68]

GABA has three methylene groups, forming an $A_2M_2X_2$ spin system, with their resonance multiplets centered at 1.89, 2.28 and 3.01 ppm. Since these resonances overlap considerably with contributions from other more abundant metabolites, selective measurement of GABA is usually carried out using spectral editing techniques to observe the multiplet group centered at 3.01 ppm.[67–71]

Aspartate (Asp)

Aspartate is an excitatory amino acid, present in the brain at approximately 1 to 2 mmol/kg_{ww}.[72] The $^{3}CH_2$ and ^{2}CH groups give a typical ABX spectral pattern consisting of a doublet-of-doublets from the CH group at 3.89 ppm and a pair of doublet-of-doublets from the protons of the $^{3}CH_2$ group at 2.65 and 2.80 ppm.

Choline (Cho), Glycerophosphorylcholine (GPC) and Phosphorylcholine (PC)

For MRS studies on tissues, the choline signal is primarily observed as a prominent singlet at 3.2 ppm that includes contributions from free choline, glycerophosphorylcholine (GPC), and phosphorylcholine (PC),[73] and it is often referred to as 'total choline'.[74–76] At short *TE*'s, overlapping resonances from phosphorylethanolamine and taurine should also be taken into account. Although phosphatidylcholine is also present at larger concentrations, no signal is observed from the component due to very short T_2 values.[77] The total NMR observable choline concentration in human brain is approximately 1–2 mmol/kg_{ww}, and known to be non-uniformly distributed.[51,52,74] The primary contributions to this total choline signal are PC and GPC, which have been measured in human brain using ^{31}P MRS in human brain at approximately 0.6 and 1 mM, respectively.[74,77] Free choline contributes little in normal brain, as it is present at <0.03 mmol/kg_{ww}, although may be significantly increased in tumors.[75] These values are in good agreement with ^{1}H studies in canine brain[78] that found PC and GPC concentrations of 0.5 and 1.3 mmol/kg_{ww}, with only a small signal from free choline.

Choline is an essential nutrient that is chiefly obtained in the form of phospholipids from the diet. It is required for synthesis of the neurotransmitter acetylcholine, and of phosphatidylcholine, a major constituent of membranes. There are 13 non-exchangeable protons in choline, nine from a trimethylamine group and four from two methylene groups. The nine protons of the trimethylamine group are magnetically equivalent and give rise to the prominent singlet at 3.19 ppm. The mutiplets from the protons of the two $^{1,2}CH_2$ groups appear at 3.50 and 4.05 ppm. The ^{14}N–H couplings between the protons of the $^{1}CH_2$ and the ^{14}N atom[79] were observed and measured to be approximately 2.6 Hz.

Glycerophosphocholine has a total of 18 protons from its glycerol and choline moieties. The trimethyl protons resonate at 3.21 ppm as a singlet. Protons of the choline-moiety $^{7}CH_2$ and $^{8}CH_2$ groups give a multiplet at 4.31 ppm and a pseudo-triplet at 3.66 ppm that overlaps with resonances of the glycerol ^{1}CH proton, respectively. The resonances from the glycerol-moiety $^{1}CH_2$ protons appear at 3.61 and 3.67 ppm as doublet-of-doublets. The remaining ^{2}CH and $^{3}CH_2$ protons resonate at 3.90, 3.87, and 3.95 ppm as multiplets. The observed ^{14}N–H couplings between $^{7}CH_2$ protons and ^{14}N were measured to be 2.67 Hz, and the ^{31}P–H couplings between the $^{3,7}CH_2$ protons and the ^{31}P were 6.03 Hz. Due to the complex spectral patterns of this metabolite, the optimization procedure failed to converge and the values presented were obtained from the NMR measurements only. This will be addressed in future work by the use of global optimization methods.

Similar to choline, phosphorylcholine also has 13 protons. A singlet seen at 3.21 ppm arises from the trimethyl protons. The protons of the $^{1}CH_2$ group resonate at 4.28 ppm as a multiplet, arising from their couplings with $^{2}CH_2$ protons, ^{31}P and ^{14}N. These ^{14}N–H and ^{31}P–H couplings were also determined, with values of 2.7 and 6.3 Hz respectively. The $^{2}CH_2$ protons give a pseudo-triplet at 3.64 ppm.

The biochemical interpretation of alterations in the MR-observed *in vivo* choline peak is complicated by the uncertainty in the metabolites contributing to the signal. Changes are generally associated with alterations of membrane composition, with increased signal associated with cancer, ischemia, head trauma, Alzheimer's disease, and multiple sclerosis, and decreased signal associated with liver disease, and stroke.[43] Decreased GPC and PE have been measured with hepatic encephalopathy,[80] attributed to the role of GPC as a cerebral osmolite. Oral choline supplements have been used for treatment of neurodegenerative disorders, based on animal studies suggesting that increased brain choline concentrations

are obtained. It has been suggested that these changes may be monitored by ^{1}H MRS,[81] though later studies indicated that any changes in the concentration of free choline may be too small for MR measurement.[74]

Creatine (Cr) and phosphocreatine (PCr)

Creatine and phosphocreatine (or creatine phosphate) are present in brain, muscle, and blood. Phosphocreatine acts as a reservoir for the generation of ATP. The synthesis of creatine takes place in the kidney and the liver. *In vivo* NMR measurements in brain observe the total of both creatine and phosphocreatine as a prominent singlet resonance from their methyl-protons, at 3.03 ppm, although it has been shown that these two contributions can be separated in spectra from rat brain at 9.4 T.[82] Concentrations in the human brain are approximately 4.0–5.5 mmol/kg$_{ww}$ for phosphocreatine, and 4.8–5.6 mmol/kg$_{ww}$ for creatine,[63] with the total creatine signal reported to be higher in gray matter, at 6.4–9.7 mM, than in white matter, at 5.2–5.7 mM.[51,52] The creatine peak is relatively stable with no changes reported with age[54] or a variety of diseases. These findings have lead to its common use as a concentration reference, though this practice should be used with caution since decreased levels are observed in tumors and stroke, and increased levels observed with myotonic dystrophy.[83]

The spectra of creatine and phosphocreatine are very similar, with their prominent singlet resonances from the methyl-protons at 3.0 ppm differing by only 0.002 ppm, and those from their methylene-protons at 3.9 ppm, differing by 0.02 ppm. In addition, their NH proton resonances at 6.6 ppm differ by 0.07 ppm, while phosphocreatine has a second NH resonance at 7.3 ppm, though these are difficult to observe *in vivo* due to their short T_2, exchange with water and strong overlap with other resonances.[84]

Ethanolamine and phosphorylethanolamine (PE)

Ethanolamine is a common alcohol moiety of phosphoglycerides, and a precursor of phosphorylethanolamine. It has two methylene groups, and these give a pair of pseudo-triplets at 3.15 and 3.82 ppm, indicating an A_2B_2 coupling network among the methylene protons. Its presence was identified in rat and gerbil brain tissue extracts.[16] In control gerbil brain extracts, its concentration was approximately 3.3 mmol/kg$_{ww}$. Ethanolamine concentration in rat brain extracts of ischemic hemisphere was reported to be significantly increased in comparison with measurements from the contralateral hemisphere of the same brain.[16]

Several other phospholipids with similar structures are also present in brain, implying that accurate characterization of these spectral regions may be difficult. However, the multiplet resonances from phosphorylethanolamine, at 3.22 and 3.98 ppm, have been included in the proton NMR spectral analysis of perchloric acid extract from biopsy specimens of the hippocampi of epilepsy patients[85] and *in vivo* rat brain.[82] In human brain, its concentration was measured at approximately 1.4 mmol/kg$_{ww}$ by ^{31}P NMR.[74,77] Increased concentrations have been observed in the rabbit hippocampus during seizures induced by kainic acid or bicuculline.[86]

D-Glucose (Glc)

Glucose is essential in the brain as a source of energy and as a precursor for a number of compounds. It is normally present at a concentration of approximately 1 mmol/kg$_{ww}$, but can be increased by plasma glucose loading to as much as 9 mmol/kg$_{ww}$.[87] Its spectrum consists of a complex multiplet pattern, though this collapses at low field strengths into two multiplets centered at 3.43 and 3.8 ppm; the latter overlaps strongly with other metabolite signals *in vivo*. Direct observation of these resonances has been demonstrated in animals at higher field strengths using one-[88] and two-dimensional[89] NMR methods, and observation of the ^{1}CH resonance of α-D-glucose at 5.23 has been demonstrated in human brain at 4.0 T.[90] At lower field strengths, changes in glucose concentration have been reported following subtraction of a baseline spectrum, enabling, for example, measurement of decreased glucose with visual stimulation[91] and measurement of its transport kinetics into the brain.[92]

Glucose contains seven non-exchangeable protons. The ^{1}CH proton exists in two different orientations relative to the ring, axial and equatorial, resulting in α and β anomers. These anomers co-exist in aqueous solutions, with an equilibrium concentration of 36% for the α anomer and 64% for the β anomer.[93] The signal from the β-D-glucose anomer is eliminated when water suppression is used.[89] The coupling pattern[94] of the α-anomer at 270 MHz proton frequency is ABC-MNO-X, where A, B, C, M, N, O and X correspond to ^{5}CH, ^{6}CH, $^{6'}$CH, ^{2}CH, ^{3}CH, ^{4}CH and ^{1}CH, whereas for the β anomer it is AB-MNOP-X, where A, B, M, N, O, P and X correspond to ^{6}CH, $^{6'}$CH, ^{5}CH, ^{4}CH, ^{3}CH, ^{2}CH and ^{1}CH. The chemical shifts and coupling constants of the two anomers have been published,[94–96] and the values presented in Table 1 are from Perkins *et al.*[94] For both the α- and β-anomers, most resonance groups occur in the range of 3.2–3.88 ppm, though differences occur for the doublet of the ^{1}CH protons which appear at 5.22 ppm for the α-anomer and at 4.63 ppm for the β-anomer.

Glutamate (Glu)

Glutamate is an amino acid with an acidic side chain. It is

the most abundant amino acid found in human brain at a concentration of approximately 12 mmol/kg_{ww}. It is known to act as an excitatory neurotransmitter, although believed to have other functions.[97,98] Cerebral glutamate concentration is reported to be increased in cerebral ischemia, hepatic encephalopathy,[99] and Rett's syndrome.[100]

Glutamate has two methylene groups and a methine group that are strongly coupled, forming an AMNPQ spin system.[101] This gives rise to a complex spectrum, resulting in low intensities of individual peaks despite its relative abundance. A previous report has presented the parameters for glutamate and glutamine measured in D_2O.[23] The signal from the single proton of the methine group is spread over as a doublet-of-doublets centered at 3.74 ppm, while the resonances from the four protons of the two methylene group are closely grouped in the 2.04–2.35 ppm range. Overlap with resonances of GABA, NAA, and glutamine complicates specific identification of their individual signal contributions *in vivo* unless some type of editing or homonuclear decoupling scheme is used.[67,100] At lower field strengths these multiplets collapse to a single resonance, leading to an apparent improvement in the observation of the combined glutamate and glutamine signals at 0.5 T relative to 1.5 T, for a PRESS acquisition at $TE = 41$ ms.[102]

Glutamine (Gln)

The amino acid glutamine is a precursor and storage form of glutamate located in astrocytes at concentrations in the range of 2–4 mM.[51] A large increase of glutamine occurs when the glutamate/glutamine cycle is altered with hyperammonemia, and in such cases glutamine is a good indicator of liver disease by monitoring it in the brain.[97,103] Glutamine is structurally similar to glutamate with two methylene groups and a methine group, and its coupling pattern is the same. A triplet from the methine proton resonates at 3.75 ppm. The multiplets from the four methylene protons are closely grouped from 2.12 to 2.46 ppm. The two amide protons appear at 6.82 and 7.53 ppm as they are chemically nonequivalent. Also, the 6.82 ppm resonance has a much higher signal intensity than the 7.53 ppm resonance because these amide protons exchange with water-protons at different rates.[104] Separation of glutamate and glutamine resonances is very difficult at lower field strengths, i.e. below 3 T, and their contributions are commonly combined when analyzing *in vivo* spectra and referred to as a 'Glx' contribution, though it has been demonstrated that these metabolites can be separately identified *in vivo* above 4 T.[105,106]

Glutathione (GSH)

Glutathione is a tripeptide made up of glycine, cysteine, and glutamate, which is present in two forms in living systems, reduced (GSH) and oxidized (GSSH). GSH is an antioxidant, essential for maintaining normal red-cell structure and keeping hemoglobin in the ferrous state. It also serves in an amino acid transport system, and is a storage form of cysteine.[107,108] It is present in the living brain almost entirely as GSH, at concentrations of 2–3 mmol/kg_{ww}, and is primarily located in astrocytes.[108] Altered GSH levels have been reported in Parkinson's disease and other neurodegenerative diseases affecting basal ganglia.[109]

The methylene protons of the glycine moiety resonate as a singlet at 3.77. The $^{7'}CH_2$ and ^{7}CH protons of the cysteine moiety form an ABX spin system with three doublet-of-doublets at 2.93, 2.98 ppm, and 4.56 ppm. From the glutamate moiety, the methine proton gives a doublet-of-doublets at 3.77 ppm, and the methylene protons give two separate multiplets at approximately 2.15 and 2.55 ppm. Since the resonances of GSH overlap with those of glutamate, glutamine, GABA, creatine, aspartate, and NAA, its unambiguous detection and quantitation is difficult from human brain *in vivo*, though it has been measured in blood.[110–112] A double quantum coherence filtering technique has been applied to the human brain and shown to enable selective observation of the cysteine-$^{7'}CH_2$ group resonances at 2.9 ppm from the overlapping resonances of GABA, creatine and aspartate.[113] In high field measurements of rat brain, GSH has been identified using a STEAM sequence with a *TE* of 2 ms.[82]

Glycerol

While glycerol is a major constituent of phospholipids and free glycerol is embedded within membrane phospholipids, proton NMR resonances from free glycerol are not observed in normal brain. However, it is an end product of membrane phospholipid degradation and increased concentrations have been associated with cerebral ischemia, seizures and traumatic brain injury.[114] Its presence has also been observed in spectra of brain homogenate, with a concentration that increases with postmortem sample preparation time.[115] The spectrum of glycerol consists of two doublet-of-doublets arising from two methylene groups and a multiplet for the CH-proton. The two doublet-of-doublets are centered at 3.55 and 3.64 ppm, and the multiplet is centered at 3.77 ppm. Since there is considerable overlap with *myo*-inositol in the 3.50 to 3.65 ppm range, care should be taken in interpreting this region for tissue homogenate studies.

Glycine (Gly)

Glycine is a simple amino acid that acts as an inhibitory

neurotransmitter and antioxidant, and is distributed throughout the brain and central nervous system. Its concentration is well regulated in the brain, being primarily synthesized from glucose through serine, with a concentration of approximately 1 mmol/kg_{ww} in humans.[116] Glycine is also readily converted into creatine. The concentration of glycine is elevated in hyperglycinemia patients[117] and tumors.[116]

Glycine has two methylene-protons that co-resonate at 3.55 ppm. For *in vivo* NMR measurements, the glycine resonance overlaps with those of myo-inositol, making unambiguous observation of glycine not possible at shorter echo times, although its presence may be inferred at longer echo times due to the cancellation of the inositol multiplet.

Histamine

The amino acid histamine is a neurotransmitter or neuromodulator, which is synthesized in the brain from histidine. It is known to be distributed non-uniformly in the brain, with highest concentrations in the hypothalamus and lowest in the cerebellum.[118] With normal concentrations of <0.1 mmol/kg_{ww} it is not observed by *in vivo* NMR, although it can be increased following histidine administration,[118] which may potentially enable detection in large tissue volumes.

Histamine has a total of six protons, two in the imidazole ring and four in its aliphatic side chain. The resonances of the imidazole ring protons depend on the solution pH, and at 7.0 pH they appear at 7.09 and 7.85 ppm. The aliphatic $^{\alpha}CH_2$ protons give a multiplet at 2.98 ppm, and the $^{\beta}CH_2$ protons appear at 3.29 ppm as a triplet.

Histidine (His)

Histidine is a neutral amino acid that is essential for the synthesis of proteins, and for the production of histamine. It is also known to act as a chelating agent. Normal concentrations are approximately 0.1 mmol/kg_{ww}. Histidine freely passes across the blood–brain barrier and its brain concentrations can be significantly increased by increasing its plasma concentrations to enable improved NMR measurement.[119,120] Increased brain histidine and histamine, especially in the hypothalmus, have been shown to occur with hepatic encepalopathy[121,122] and histidinemia,[119,123] a defect of amino acid metabolism.

Histidine has five protons, out of which two protons are in a five-membered imidazole ring and the remaining three are in its aliphatic side chain. In addition, it has four water-exchangeable amine protons that are normally not observed at physiological temperature. There is a pH dependence of the resonances at 7.8 and 7.1 ppm,[10] enabling pH measurement *in vivo* using ^{1}H NMR.[120,124]

Homocarnosine

Homocarnosine is a dipeptide that consists of histidine and GABA. It was first identified in bovine brain[125] and later in human brain, CSF and urine.[126] In human brain, its concentration ranges from 0.3 to 0.6 mmol/kg_{ww}.[127–129] Elevated levels in the CSF and brain tissues are characteristic of homocarnosinosis, a metabolic disorder associated with spastic paraplegia, progressive mental retardation, and retinal pigmentation, that is caused by a deficiency of the homocarnosine-metabolizing enzyme, homocarnosinase.[123,127,128,130]

The histidine–imidazole CH-protons in homocarnosine resonate at 8.08 and 7.08 ppm and are sensitive to local chemical environment, making this one of the possible metabolites for measuring intracellular pH.[131] The α-proton of its histidine moiety gives a six-line multiplet at 4.47 ppm and its β-protons give two doublet-of-doublets at 3.19 and 3.00 ppm. The protons of the three methylene groups of its GABA moiety are very similar to those of GABA, with multiplet groups at 2.96, 2.37 and 1.89 ppm. The spin–spin couplings of the groups contributing to the region upfield from water are complex, and difficult to determine by our spectral optimization procedure. Since the concentration of homocarnosine in normal human brain is low and these resonances do not typically contribute a measurable signal, these parameters remain undetermined.

Myo-inositol (m-Ins)

Of the nine isomers of inositol,[132] *myo*-inositol is the predominate form found in tissue.[9] This compound can be detected in brain using shorter-*TE* acquisitions, although the signal normally attributed to *myo*-inositol may also contain smaller contributions from inositol monophosphate, inositol polyphosphates[97] and glycine. The function of *myo*-inositol is not well understood, although it is believed to be an essential requirement for cell growth, an osmolite, and a storage form for glucose.[97] It has been proposed as a glial marker.[133] Normal concentrations range from 4 to 8 mmol/kg_{ww},[50,51] and altered levels have been associated with Alzheimer's disease,[134] hepatic encephalopathy[135] and brain injury.[136]

Myo-inositol is a cyclic sugar alcohol that has six protons. This compound gives four groups of resonances. A doublet-of-doublet centered at 3.52 ppm and a triplet at 3.61 ppm are the two prominent multiplets each corresponding to two protons. A triplet at 3.27 ppm is typically hidden under choline, and another at 4.05 ppm is typically not observed because of water suppression.

Scyllo-inositol (s-Ins)

Scyllo-inositol is the second most abundant isomer of inositol that is found in mammals although its presence appears to be species dependent as it has been found in brains of human, bovine, and sheep, but not in rats.[137] It gives a singlet resonance at 3.34 ppm, and in humans its concentration is reported to be closely coupled with that of *myo*-inositol, with a 12:1 ratio,[137] though elevated *scyllo*-inositol concentration has been reported.[138] While the presence of *scyllo*-inositol in perchloric acid extracts has been confirmed, these studies must also take into account possible misidentification due to methanol,[139] which may be a contaminant of the extract procedure.

Lactate (Lac)

Lactate is the end product of anaerobic glycolysis, normally present in brain tissue at low concentrations[140] and therefore generally not observed by *in vivo* MRS studies. Increased concentrations occur rapidly following hypoxia and its observation is therefore of great interest for clinical MRS studies in situations where blood flow may be impaired, such as stroke, trauma or tumors,[43] though its presence can be highly variable. It is also found in necrotic tissue or fluid-filled cysts. Transient increases of lactate have also been observed in human brain following functional activation and hyperventilation.[141,142]

The methyl and methine groups of lactate form an A_3X spin system and detection is commonly carried out via the doublet from the methyl group, at 1.31 ppm. However, since this spectral region is frequently complicated by the presence of lipid resonances, several lactate editing sequences have been proposed[143] and observation is commonly performed at longer *TE* times where the relative lipid contribution is diminished. The methine group quartet at 4.09 ppm is typically not observed *in vivo* due to its close proximity to water.

Phenylalanine (Phe)

Phenylalanine is an aromatic amino acid that has a phenyl ring in place of a hydrogen atom in the alanine-methyl group. It is known to be a precursor for catecholamine synthesis, and normally present in human brain at approximately 0.2 mM.[144] Its concentration is elevated in phenylketonuria (PKU), an inborn error of phenylalanine metabolism, and can reach 5 mM. In PKU patients, the hydroxylation of phenylalanine to tyrosine is disturbed due to an absence or deficiency of the liver enzyme phenylalanine hydroxylase, or rarely, of its tetrahydrobiopterin cofactor.[123,145] Untreated PKU patients are characterized by impairment of brain development, severe mental retardation, microcephaly, epilepsy and other neurological disorders. In recent years, proton MRS has been used to identify and quantify phenylalanine in PKU patients,[144,146–152] using short-*TE* measurements.

Phenylalanine has eight hydrogen atoms, five in the phenyl ring and three in the aliphatic side chain. Its high-resolution spectrum contains a multiplet spread between 7.30 and 7.45 ppm from three groups of chemically and magnetically nonequivalent protons in the phenyl ring. The α-proton gives a doublet-of-doublets at 3.98 ppm, and the β-protons give rise to two doublet-of-doublets centered at 3.11 and 3.28 ppm. The T_2 value reported for the downfield phenylalanine resonances in human brain was 65 ms.[148]

Pyruvate

Pyruvate, together with ATP, is an end produce of glycolysis, following which it enters the Krebs cycle under aerobic conditions, or forms lactate under anaerobic conditions. While it may be clearly identified from a singlet resonance at 2.36 ppm in high-resolution spectra of plasma[17] or in brain extract studies, the normal concentration is under 0.2 mmol/kg_{ww} and *in vivo* observation has been limited to increased concentrations in cystic lesions.[153] This resonance is very close to that of succinate (at 2.39 ppm), reported in similar cases.[36]

Serine (Ser)

Serine is an amino acid that is incorporated in many proteins, interchangeable with glycine, and present throughout the brain at a concentration of approximately 0.4 mmol/kg_{ww}. It has ^2CH and $^3CH_2$ groups, forming an ABX spin system. The ^2CH and $^3CH_2$ protons give three closely spaced doublet-of-doublets at 3.83, 3.94 and 3.98 ppm, respectively.

Succinate (Suc)

A component of the citric acid cycle, succinate is present in brain at approximately 0.5 mmol/kg_{ww}.[72] Although present at only low concentration, it contains four protons from two methylene groups that all contribute to a singlet at 2.39 ppm. In conventional *in vivo* one-dimensional NMR experiments, this signal overlaps with resonances of glutamate and glutamine. Increased succinate has been reported in human brain in brain abcesses,[36] although this may also indicate the presence of pyruvate.

Taurine (Tau)

Taurine (2-aminoethanesulfonic acid) is an amino acid that is reported to have a number of biological functions,

including osmoregulation and modulation of the action of neurotransmitters.[154] It is found at high concentration at the time of birth and decreases with age, to a concentration of approximately 1.5 mM. It is chiefly obtained from food, although it may also be synthesized within in the brain from other sulfur-containing amino acids. It has two adjacent methylene groups, forming an AA′XX′ spin system, though separation between the non-equivalent protons is very small and it can be considered as an A_2X_2 system, with a spectrum containing two triplets at 3.25 and 3.42 ppm. For *in vivo* studies at lower field strengths, these resonances commonly overlap with the resonances from *myo*-inositol and choline, and a selective irradiation technique[67] or double quantum filter has been demonstrated to improve observation of taurine.[154] Direct observation in human brain at 1.5 T has been reported following oral consumption leading to increased concentrations.[155]

Threonine (Thr)

Threonine is a large neutral amino acid, essential to the diet, and efficiently transported through the blood–brain barrier. In the brain, it can be converted into glycine and serine, although it is not believed to have a direct effect on brain function.[156] Normal concentrations are approximately 0.3 mmol/kg_{ww}.

Threonine has five water non-exchangeable protons from a CH_3 and two CH groups following an A_3MX spectral pattern. The ^{2}CH proton gives a doublet at 3.58 ppm, and the ^{3}CH proton resonates at 4.25 ppm to give an eight-line multiplet because of its coupling with the ^{2}CH and CH_3 protons. The $^4CH_3$ protons give a doublet at 1.32 ppm because of their coupling with the ^{3}CH proton.

Tryptophan (Trp)

Tryptophan is an essential amino acid that is necessary for the production of serotonin, an important neurotransmitter. Normally present at approximately 0.03 mmol/kg_{ww}, the brain concentration can be altered by tryptophan consumption. Higher tryptophan levels lead to an increase in serotonin synthesis by approximately a factor of two, which has lead to its investigation for treatment of mild insomnia, and as a mild antidepressant,[156] as well as to its association with eosinophilia myalgia syndrome, inadvertently caused by toxic by-products of the commercial production of L-tryptophan.[157] Increased brain tryptophan also results from hepatic encephalopathy.[158]

Tryptophan has eight protons. The ^{2}CH proton gives a singlet at 7.31 ppm, and the four phenyl ring protons give two multiplets centered at 7.20 and 7.28 ppm. The three aliphatic side chain protons give three doublet-of-doublets between 3.29 and 4.05 ppm. Although tryptophan is normally present at only low concentration, the resonances of the indole ring may combine sufficiently to provide an identifiable signal at 1.5 T.[84]

Tyrosine (Tyr)

Tyrosine is an essential neutral amino acid that can be synthesized from phenylalanine, and a precursor of the neurotransmitters epinephrine, norepinephrine, and dopamine. Normal brain concentrations are in the range of 0.06 mmol/kg_{ww}, although it can be increased following oral consumption as well as by hepatic encephalopathy. It may have some clinical use for treatment of Parkinson's disease and depression.[159]

Tyrosine has seven water non-exchangeable protons, four from the phenyl ring and three from its aliphatic side chain. The four phenyl ring protons give a multiplet spread between 6.89 and 7.19 ppm. The CH and CH_2 aliphatic protons of an ABX spin system give three doublet-of-doublets between 3.04 and 3.93 ppm.

Valine (Val)

Valine is an essential amino acid necessary for protein synthesis. Its uptake in the brain is higher than all other amino acids. It has eight protons present in two CH_3 and two CH groups. The spectrum consists of two doublets from the two methyl protons that overlap with resonances of leucine and isoleucine in the range of 0.95–1.05 ppm. For *in vivo* studies, this group of resonances appears as a single broad line that is difficult to distinguish from macromolecular resonances at this same position.[21] A complex multiplet appears at 2.26 ppm from the ^{3}CH proton which overlaps with resonances of GABA and glutamate. The ^{2}CH proton gives a doublet at 3.60 ppm that merges with resonances of myo-inositol. Hypervalinemia and branched-chain ketonuria[123] are some of the diseases in which valine level gets elevated, and increased concentrations have also been observed in brain abcesses.[36,65]

Rat brain tissue PCA extract studies

In Fig. 3 are shown data and fit results for a spectrum of rat brain PCA extract. Two sections of the spectrum are shown, each covering a different ppm range upfield from water. To obtain the result shown, it was necessary to apply minor adjustments to the chemical shift values of several resonance groups from the values shown in Table 1, while no differences in the splittings of any multiplet groups were observed. The average value of the adjustments applied to the chemical shifts was only 0.006 ppm, while the maximum applied shift was 0.024 ppm, for the 2.65 ppm multiplet of aspartate. Both

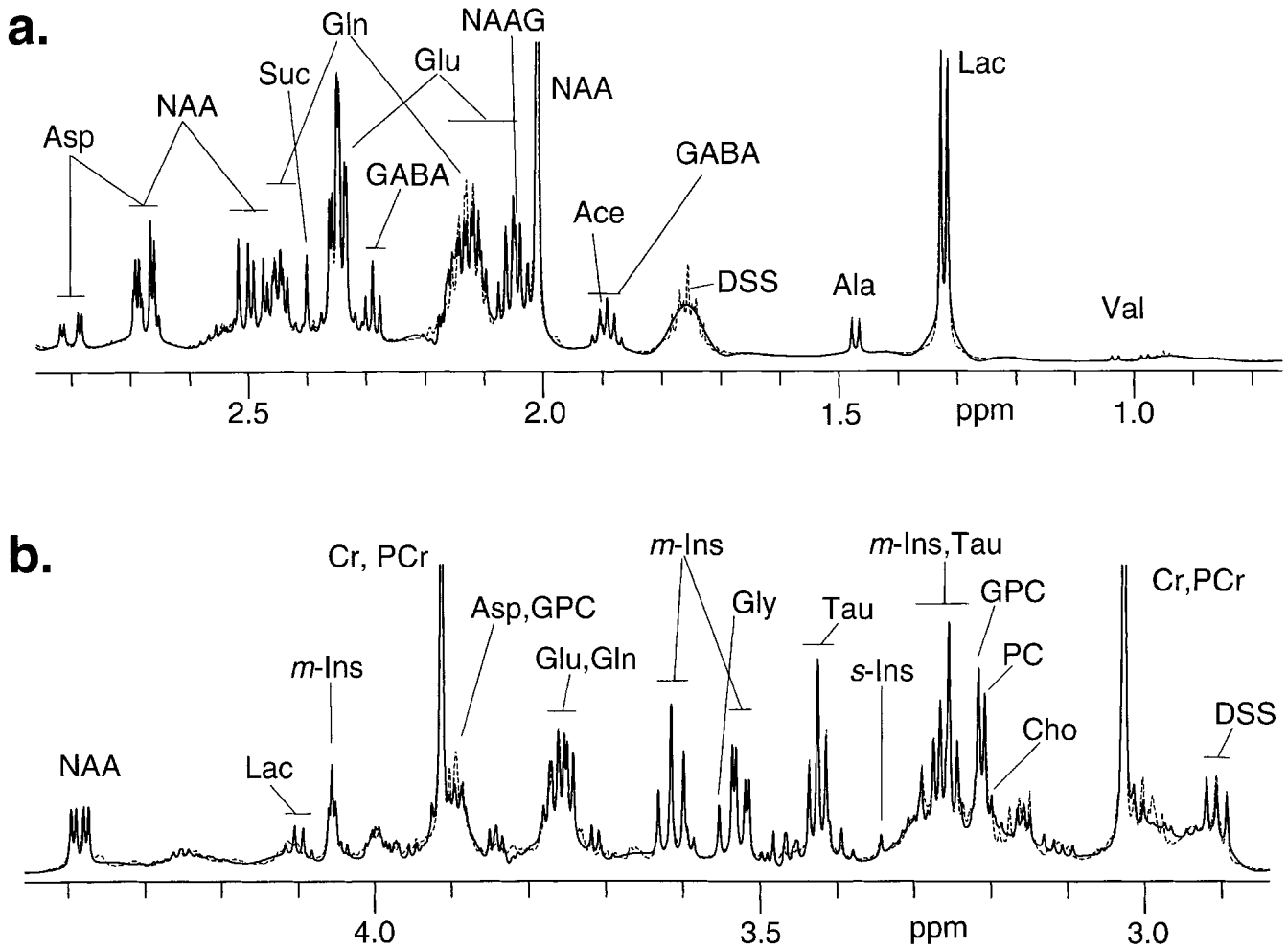

Figure 3. High-resolution ^{1}H spectrum for PCA extract of rat brain obtained at 600 MHz (dashed line), together with results of the parametric spectral analysis using the NMR parameters determined for each compound (solid line). Data are shown for two spectral regions from: (a) 0.75 to 2.85 ppm; and (b) 2.85 to 4.45 ppm. Note that the vertical scale has been increased, resulting in truncation of the larger peaks. The metabolite assignments are identified using abbreviations used in the text

positive and negative shifts were used and no trends could be discerned. The requirement for this shift is attributed to possible differences in the sample conditions of the PCA extract in comparison with the solution measurements and binding effects in the PCA extract solution. This observation indicates that for parametric analysis of high-resolution spectra such as that shown in Fig. 3, it is necessary to include in the model the ability to fractionally alter the chemical shifts of individual resonance groups. The relative resonance intensities and phases of the spectral model would remain unchanged. With the exception of pH dependent resonances, it is anticipated that this will not be necessary for *in vivo* data obtained at lower field strengths where linewidths typically greatly exceed these observed differences in shift values.

For the most part, the correspondence between the resonance positions in the data and the fitted spectrum in the region upfield from water was excellent. The residual of the fit was dominated by differences in the lineshape, as some asymmetry of the experimental lineshape was evident, differing from the Lorentz–Gauss model (dominated by Lorentzian) used for the fit. The fit included correct identification of 33 metabolites. The multiplet group seen at 1.76 ppm of the data shown in Fig. 3(a) (dashed line) is from DSS, which was not included in the spectral model, and the fit result (solid line) therefore shows only the fitted baseline signal in this region. It was, however, necessary to include the pseudotriplet from DSS at 2.90 ppm in the model. The following additional differences between the data and the fit result were noted:

1. Increased linewidths were observed for the lactate quartet at 4.1 ppm, and for the NAA doublet-of-doublets at 4.38 ppm. This may be due to binding effects, or for NAA, coupling with nitrogen.
2. At the position of the singlet resonance from *scyllo*-inositol, measured at 3.340 in D_2O solution, two overlapping resonances appeared of equal amplitude at 3.3432 and 3.345 ppm. This additional

resonance is unidentified, but could be due to methanol contamination as described by Michaelis and Frahm,[139] who have identified *scyllo*-inositol at 3.350 ppm and methanol at 3.354 ppm.

3. Difficulty in fitting the region between 2.1 and 2.15 ppm was observed. This may indicate the presence of additional uncharacterized resonances, though could also indicate the presence of different rotamer distributions of glutamine between the solution measurement and the extract solutions. Other regions where exact alignment of model spectra and the data were not obtained were primarily associated with ethanolamine and phosphorylethanolamine, indicating that other similar phospholipids may be present, of which glycerophosphoryl-ethanolamine is a likely candidate.[77]

The fit of the region downfield from water remains incomplete due to the presence of a number of unassigned resonances. However, these were present at low amplitude, and likely to originate from metabolites present at low concentrations that are not included in this review. Resonance groups that were correctly fit included those of NAA, ATP, α-glucose, histidine, phenylalanine, tryptophan and tyrosine.

Additional spectral fits were performed for *in vivo* results obtained in rat brain at 9.4 T (data courtesy of R. Gruetter, and shown elsewhere[82]). An excellent fit was obtained using 23 metabolites (results not shown). Due to the broader linewidth present in these *in vivo* data, differences between the resonance positions determined from the model functions derived from the solution spectra were barely evident. Nevertheless, it was felt that the quality of the fit did benefit from small changes, on the order of 0.004 ppm, to the shift positions of 5 multiplet groups, and a larger shift of +0.01 ppm for all groups *myo*-inositol. Coincidentally, this same shift was applied to the 3.27 and 3.52 ppm groups of *myo*-inositol for the extract spectrum. It is speculated that this may reflect binding of *myo*-inositol to proteins and membranes, though since greater spectral overlap is present in these data, in comparison to the extract study, the presence of additional resonances not included in the model cannot be discounted. These findings are preliminary and additional work is necessary to confirm these observations. No significant differences between the fit and the data were apparent, indicating that all major metabolite contributions were accounted for.

CONCLUSIONS

A detailed compilation of proton chemical shifts and coupling constants for brain metabolites has been presented. Most of these values have been obtained using experimental measurements carried out for a consistent set of experimental conditions. A primary aim of this report has been to make available the *a priori* spectral information necessary for generating by computer simulation the basis functions required for parametric spectral analysis procedures. By incorporating knowledge of the metabolite structure, spectral parameters (Table 1), and experimental conditions, a computer simulation procedure can be used to generate a complete list of relative frequencies, amplitudes, and phases of all resonances for each metabolite. In addition, typical concentration values in human brain (Table 2) may be used as starting values of an estimation procedure, following appropriate correction for spin relaxation and acquisition parameters. The accuracy of this data, and of the spectral simulation approach, has been verified by comparison of simulation results with experimental spectra from individual metabolites in solution and by analysis of spectra obtained from rat brain extract.

A finding of this study was the observation of small differences between the chemical shift values measured in solution, from those observed in PCA extract and *in vivo*. No differences between the *J*-coupling constants were observed. Changes in chemical shifts of several groups are expected due to differences in pH, and although this was controlled for, changes of the extract solution may have occurred between preparation and measurement. Additionally, chemical shift changes may reflect binding effects and ionic strength, as well as the solvent isotope effect, the mechanism of which is not well understood. Nevertheless, the observed differences were small, for the most part being on the order of the sampling resolution. However, this implies that for application of the parametric spectral analysis approach to high-resolution spectra obtained at high field strengths, it is necessary to allow for frequency shifts of the individual multiplet groups, with appropriate constraints. For analysis of spectra obtained at lower field strengths and *in vivo*, this requirement is considerably relaxed, with the exception of strongly pH-dependent resonances.

One limitation that was encountered in this study was the inability of the spectral optimization procedure to reliably converge to the optimum solution for a few of the metabolites. For these cases, we have therefore either supplemented our measurements with values obtained from previously published reports or presented our best available result determined from one- or two-dimensional measurements. It is anticipated that an improvement of the spectral optimization procedure will be possible in the future with the development of a more global optimization algorithm, and that continued refinement of the measured parameters will be carried out. As further information is obtained it will be made available at URL http://www.sf.med.va.gov/mrs/, or may be obtained from the authors.

In this study, no attempt was made to quantify the relative populations of different conformers and rotamers, and the reported chemical shifts and couplings correspond to the equilibrium populations found in

solution for the conditions used. Additional limitations of the information presented are that potential spectral changes due to a number of physical variables are not accounted for. For example, changes in chemical shifts caused by the local conditions of pH and temperature, variations of relative line widths due to differences in relaxation rates between molecular groups, and amplitude changes due to magnetization transfer effects.[160] In principle, these variables can be accounted for by including them as independent parameters in the modeling procedure, following suitable characterization of the dependencies of these parameters. An alternative approach is to relax the associated parameter constraints, for example to allow for changes of those resonances frequencies for which variations are anticipated.

Acknowledgements

This work was supported by PHS grant AG12119 (A.A.M.). We thank Dr Vladimir J. Basus for assisting with the NMR facilities and advice with the NMR studies, Vinh Lam for assistance with spectroscopic measurements, Dr Brian Soher for assistance with the automated spectral analysis program, Dr Natalie Serkova for providing us with the PCA extract preparation, and Dr Rolf Gruetter for making their data available to us.

REFERENCES

1. De Graaf AA, Bovee WMMJ. Improved quantification of *in vivo* 1H NMR spectra by optimization of signal acquisition and processing and by incorporation of prior knowledge into the spectral fitting. *Magn. Reson. Med.* 1990; **15**: 305–319.
2. Provencher SW, Estimation of metabolite concentrations from localized *in vivo* proton NMR spectra. *Magn. Reson. Med.* 1993; **30**: 672–679.
3. Slotboom J, Boesch C, Kreis R. Versatile frequency domain fitting using time domain models and prior knowledge. *Magn. Reson. Med.* 1998; **39**: 899–911.
4. Young K, Govindaraju V, Soher BJ, Maudsley AA. Automated spectral analysis I: formation of *a priori* information by spectral simulation. *Magn. Reson. Med.* 1998; **40**: 812–815.
5. Soher BJ, Young K, Govindaraju V, Maudsley AA. Automated spectral analysis III: Application to in vivo proton MR spectroscopy and spectroscopic imaging. *Magn. Reson. Med.* 1998; **40**: 822–831.
6. Behar KL, den Hollander JA, Stromski ME, Ogino T, Shulman RG, Petroff OA, Prichard JW. High-resolution 1H nuclear magnetic resonance study of cerebral hypoxia *in vivo*. *Proc. Natl Acad. Sci. USA* 1983; **80**: 4945–4948.
7. Arús C, Bárány M. ^{1}H NMR of intact tissues at 11.1 T. *J. Magn. Reson.* 1984; **57**: 519–525.
8. Arús C, Chang Y-C, Bárány M. Proton nuclear magnetic resonance spectra of excised rat brain. Assignment of resonances. *Physiol. Chem. Phys. Med. NMR* 1985; **17**: 23–33.
9. Cerdán S, Parrilla R, Santoro J, Rico M. 1H NMR detection of cerebral *myo*-inositol. *FEBS Lett.* 1985; **187**: 167–172.
10. Fan TW, Higashi RM, Lane AN, Jardetzky O. Combined use of 1H-NMR and GC-MS for metabolite monitoring and *in vivo* 1H-NMR assignments. *Biochim. Biophys. Acta* 1986; **882**: 154–167.
11. Sze DY, Jardetzky O. Determination of metabolite and nucleotide concentrations in proliferating lymphocytes by 1H-NMR of acid extracts. *Biochim. Biophys. Acta* 1990; **1054**: 181–197.
12. Michaelis T, Merboldt KD, Hänicke W, Gyngell ML, Bruhn H, Frahm J. On the identification of cerebral metabolites in localized 1H NMR spectra of human brain *in vivo*. *NMR Biomed.* 1991; **4**: 90–98.
13. Behar KL, Ogino T. Assignment of resonances in the 1H spectrum of rat brain by two-dimensional shift correlated and *J*-resolved NMR spectroscopy. *Magn. Reson. Med.* 1991; **17**: 285–303.
14. van Zijl PCM, Moonen CTW. *In situ* changes in purine nucleotide and *N*-acetyl concentrations upon inducing global ischemia in cat brain. *Magn. Reson. Med.* 1993; **29**: 381–385.
15. Ryner LN, Sorenson JA, Thomas MA. Localized 2D *J*-resolved 1H MR spectroscopy: strong coupling effects *in vitro* and *in vivo*. [Published erratum appears in Magn. Reson. Imag. 1995; 13: 1043]. *Magn. Reson. Imag.* 1995; **13**: 853–869.
16. Smart SC, Fox GB, Allen KL, Swanson AG, Newman MJ, Swayne GT, Clark JB, Sales KD, Williams SC. Identification of ethanolamine in rat and gerbil brain tissue extracts by NMR spectroscopy. *NMR Biomed.* 1994; **7**: 356–365.
17. Wevers RA, Engelke U, Heerschap A. High-resolution 1H-NMR spectroscopy of blood plasma for metabolic studies. [See comments.] *Clin. Chem.* 1994; **40**: 1245–1250.
18. Wevers RA, Engelke U, Wendel U, de Jong JG, Gabreëls FJ, Heerschap A. Standardized method for high-resolution 1H-NMR of cerebrospinal fluid. *Clin. Chem.* 1995; **41**: 744–751.
19. Slotboom J, Mehlkopf AF, Bovee WMMJ. The effects of frequency-selective RF pulses on *J*-coupled spin-1/2 systems. *J. Magn. Reson. Ser. A* 1994; **108**: 38–50.
20. Yablonskiy DA, Neil JJ, Raichle ME, Ackerman JJ. Homonuclear J coupling effects in volume localized NMR spectroscopy: pitfalls and solutions. *Magn. Reson. Med.* 1998; **39**: 169–178.
21. Behar KL, Rothman DL, Spencer DD, Petroff OAC. Analysis of macromolecule resonances in 1H NMR spectra of human brain. *Magn. Reson. Med.* 1994; **32**: 294–302.
22. Young K, Soher BJ, Maudsley AA. Automated spectral analysis II: application of wavelet shrinkage for characterization of non-parameterized signals. *Magn. Reson. Med.* 1998; **40**: 816–821.
23. Govindaraju V, Basus VJ, Matson GB, Maudsley AA. Measurement of chemical shifts and coupling constants for glutamate and glutamine. *Magn. Reson. Med.* 1998; **39**: 1011–1013.
24. Govindaraju V, Young K, Matson GB, Maudsley AA. Optimization of acquisition sequence parameters by spectral simulation (submitted).
25. Rigaudy J, Klesney SP, eds. Nomenclature of Organic Chemistry, Pergamon Press, Oxford (1979).
26. Wüthrich K, NMR of Proteins and Nucleic Acids, Wiley, New York (1986).
27. Wishart DS, Bigam CG, Yao J, Abildgaard F, Dyson HJ, Oldfield E, Markley JL, Sykes BD. 1H, 13C and 15N chemical shift referencing in biomolecular NMR. *J. Biomol. NMR* 1995; **6**: 135–140.
28. Smith SA, Levante TO, Meier BH, Ernst RR. Computer simulations in magnetic resonance. An object-oriented programming approach. *J. Magn. Reson. Ser. A* 1994; **106**: 75–105.
29. Serkova N, Brand A, Christians U, Leibfritz D. Evaluation of the effects of immunosuppressants on neuronal and glial cells *in vitro* by multinuclear magnetic resonance spectroscopy. *Biochim. Biophys. Acta* 1996; **1314**: 93–104.
30. Middlehurst CR, King GF, Beilharz GR, Hunt GE, Johnson GFS, Kuchel PW. Studies of rat brain metabolism using proton nuclear magnetic resonance: spectral assignments and monitoring of prolidase, acetylcholinesterase and glutaminase. *J. Neurochem.* 1984; **43**: 1561–1567.
31. Petroff OAC, Spencer DD, Alger JR, Prichard JW. High-field proton magnetic resonance spectroscopy of human cerebrum obtained during surgery for epilepsy. *Neurology* 1989; **39**: 1197–1202.
32. Urenjak J, Williams SR, Gadian DG, Noble M. Proton nuclear magnetic resonance spectroscopy unambiguously identifies different neural cell types. *J. Neurosci.* 1993; **13**: 981–989.
33. Martin M, Merle M, Labouesse J, Canioni P. Postnatal decrease of acetate concentration in rat cerebellum. *J. Neurosci. Res.* 1994; **37**: 103–107.
34. Florian CL, Preece NE, Bhakoo KK, Williams SR, Noble M. Characteristic metabolic profiles revealed by 1H NMR spec-

troscopy for three types of human brain and nervous system tumours. *NMR Biomed.* 1995; **8**: 253–264.
35. Peeling J, Wong D, Sutherland GR. Nuclear magnetic resonance study of regional metabolism after forebrain ischemia in rats. *Stroke* 1989; **20**: 633–640.
36. Kim SH, Chang KH, Song IC, Han MH, Kim HC, Kang HS, Han MC. Brain abscess and brain tumor: discrimination with *in vivo* H-1 MR spectroscopy. *Radiology* 1997; **204**: 239–245.
37. Davies SE, Newcombe J, Williams SR, McDonald WI, Clark JB. High resolution proton NMR spectroscopy of multiple sclerosis lesions. *J. Neurochem.* 1995; **64**: 742–748.
38. Martin M, Labouesse J, Canioni P, Merle M. *N*-Acetyl-L-aspartate and acetate 1H NMR signal overlapping under mild acidic pH conditions. *Magn. Reson. Med.* 1993; **29**: 692–694.
39. Birken DL, Oldendorf WH. *N*-Acetyl-L-aspartic acid: a literature review of a compound prominent in 1H-NMR spectroscopic studies of brain. *Neurosci. Biobehav. Rev.* 1989; **13**: 23–31.
40. Miyake M, Kakimoto Y, Sorimachi M. A gas chromatographic method for the determination of *N*-acetyl-L-aspartic acid, *N*-acetyl-alpha-aspartylglutamic acid and beta-citryl-L-glutamic acid and their distributions in the brain and other organs of various species of animals. *J. Neurochem.* 1981; **36**: 804–810.
41. Baslow MH. A review of phylogenetic and metabolic relationships between the acylamino acids, *N*-acetyl-L-aspartic acid and *N*-acetyl-L-histidine, in the vertebrate nervous system. *J. Neurochem.* 1997; **68**: 1335–1344.
42. Tsai G, Coyle JT. *N*-Acetylaspartate in neuropsychiatric disorders. *Prog. Neurobiol.* 1995; **46**: 531–540.
43. Rudkin TM, Arnold DL. Proton magnetic resonance spectroscopy for the diagnosis and management of cerebral disorders. *Arch. Neurol.* 1999; **56**: 919–926.
44. Simmons ML, Frondoza CG, Coyle JT. Immunocytochemical localization of N-acetyl-aspartate with monoclonal antibodies. *Neuroscience* 1991; **45**: 37–45.
45. Urenjak J, Williams SR, Gadian DG, Noble M. Specific expression of *N*-acetylaspartate in neurons, oligodendrocyte-type-2 astrocyte progenitors, and immature oligodendrocytes *in vitro*. *J. Neurochem.* 1992; **59**: 55–61.
46. Brulatout S, Méric P, Loubinoux I, Borredon J, Corrèze JL, Roucher P, Gillet B, Bérenger G, Beloeil JC, Tiffon B, Mispelter J, Seylaz J. A one-dimensional (proton and phosphorus) and two-dimensional (proton) *in vivo* NMR spectroscopic study of reversible global cerebral ischemia. *J. Neurochem.* 1996; **66**: 2491–2499.
47. De Stefano N, Matthews PM, Arnold DL. Reversible decreases in *N*-acetylaspartate after acute brain injury. *Magn. Reson. Med.* 1995; **34**: 721–727.
48. Wittsack HJ, Kugel H, Roth B, Heindel W. Quantitative measurements with localized 1H MR spectroscopy in children with Canavan's disease. *J. Magn. Reson. Imag.* 1996; **6**: 889–893.
49. Arús C, Chang Y-C and Bárány M. *N*-Acetylaspartate as an intrinsic thermometer for ^{1}H NMR of brain slices. *J. Magn. Reson.* 1985; **63**: 376–379.
50. Kreis R. Quantitative localized 1H MR spectroscopy for clinical use. *Prog. Magn. Reson. Spectrosp.* 1997; **31**: 155–195.
51. Pouwels PJ, Frahm J. Regional metabolite concentrations in human brain as determined by quantitative localized proton MRS. *Magn. Reson. Med.* 1998; **39**: 53–60.
52. Wang Y, Li SJ. Differentiation of metabolic concentrations between gray matter and white matter of human brain by *in vivo* 1H magnetic resonance spectroscopy. *Magn. Reson. Med.* 1998; **39**: 28–33.
53. Lim KO, Spielman DM. Estimating NAA in cortical gray matter with applications for measuring changes due to aging. *Magn. Reson. Med.* 1997; **37**: 372–377.
54. Saunders DE, Howe FA, van den Boogaart A, Griffiths JR, Brown MM. Aging of the adult human brain: *In vivo* quantitation of metabolite content with proton magnetic resonance spectroscopy. *J. Magn. Reson. Imaging* 1999; **9**: 711–716.
55. Curatolo A, d'Arcangelo P, Lino A, Brancati A. Distribution of N-acetyl-aspartic and N-acetyl-aspartyl-glutamic acids in nerve tissue. *J. Neurochem.* 1965; **12**: 339–342.
56. Ory-Lavollée L, Blakely RD, Coyle JT. Neurochemical and immunocytochemical studies on the distribution of *N*-acetyl-aspartylglutamate and *N*-acetyl-aspartate in rat spinal cord and some peripheral nervous tissues. *J. Neurochem.* 1987; **48**: 895–899.
57. d'Arcangelo P, Brancati A. Distribution of *N*-acetylaspartate, *N*-acetylaspartylglutamate, free glutamate and aspartate following complete mesencephalic transection in rat neuraxis. *Neurosci. Lett.* 1990; **114**: 82–88.
58. Koller KJ, Zaczek R, Coyle JT. *N*-Acetyl-aspartyl-glutamate: regional levels in rat brain and the effects of brain lesions as determined by a new HPLC method. *J. Neurochem.* 1984; **43**: 1136–1142.
59. Pouwels PJ, Frahm J. Differential distribution of NAA and NAAG in human brain as determined by quantitative localized proton MRS. *NMR Biomed.* 1997; **10**: 73–78.
60. Coyle JT. The nagging question of the function of *N*-acetylaspartylglutamate. *Neurobiol. Dis.* 1997; **4**: 231–238.
61. Passani LA, Vonsattel JP, Carter RE, Coyle JT. *N*-Acetylaspartylglutamate, *N*-acetylaspartate, and *N*-acetylated alpha-linked acidic dipeptidase in human brain and their alterations in Huntington and Alzheimer's diseases. *Mol. Chem. Neuropathol.* 1997; **31**: 97–118.
62. Holowenko D, Peeling J, Sutherland G. 1H NMR properties of *N*-acetylaspartylglutamate in extracts of nervous tissue of the rat. *NMR Biomed.* 1992; **5**: 43–47.
63. Erecianska M, Silver IA. ATP and brain function. *J. Cereb. Blood Flow Metab.* 1989; **9**: 2–19.
64. Son TD, Chachaty C. Proton NMR and spin lattice relaxation study of nucleoside di-and triphosphates in neutral aqueous solutions. *Biochim. Biophys. Acta* 1977; **500**: 405–418.
65. Poptani H, Gupta RK, Jain VK, Roy R, Pandey R. Cystic intracranial mass lesions: possible role of *in vivo* MR spectroscopy in its differential diagnosis. *Magn. Reson. Imag.* 1995; **13**: 1019–1029.
66. Higuchi T, Graham SH, Fernandez EJ, Rooney WD, Gaspary HL, Weiner MW, Maudsley AA. Effects of severe global ischemia on *N*-acetylaspartate and other metabolites in the rat brain. *Magn. Reson. Med.* 1997; **37**: 851–857.
67. Rothman DL, Behar KL, Hetherington HP, Shulman RG. Homonuclear 1H double resonance difference spectroscopy of the rat brain *in vivo*. *Proc. Natl Acad. Sci. USA* 1984; **81**: 6330–6334.
68. Petroff OA, Rothman DL. Measuring human brain GABA *in vivo*: effects of GABA-transaminase inhibition with vigabatrin. *Mol. Neurobiol.* 1998; **16**: 97–121.
69. Rothman DL, Petroff OA, Behar KL, Mattson RH. Localized 1H NMR measurements of gamma-aminobutyric acid in human brain *in vivo*. *Proc. Natl Acad. Sci. USA* 1993; **90**: 5662–5666.
70. Wilman AH, Allen PS. Yield enhancement of a double-quantum filter sequence designed for the edited detection of GABA. *J. Magn. Reson. Ser. B* 1995; **109**: 169–174.
71. Keltner Wald LL, Frederick BD, Renshaw PF. *In vivo* detection of GABA in human brain using a localized double-quantum filter technique. *Magn. Reson. Med.* 1997; **37**: 366–371.
72. Klunk WE, Xu C, Panchalingam K, McClure RJ, Pettegrew JW. Quantitative 1H and 31P MRS of PCA extracts of postmortem Alzheimer's disease brain. *Neurobiol. Aging* 1996; **17**: 349–357.
73. Miller BL. A review of chemical issues in 1H NMR spectroscopy: *N*-Acetyl-L-aspartate, creatine and choline. *NMR Biomed.* 1991; **4**: 47–52.
74. Tan J, Blüml S, Hoang T, Dubowitz D, Mevenkamp G, Ross B. Lack of effect of oral choline supplement on the concentrations of choline metabolites in human brain. *Magn. Reson. Med.* 1998; **39**: 1005–1010.
75. Miller BL, Chang L, Booth R, Ernst T, Cornford M, Nikas D, McBride D, Jenden DJ. *In vivo* 1H MRS choline: correlation with in vitro chemistry/histology. *Life Sci.* 1996; **58**: 1929–1935.
76. Michaelis T, Merboldt KD, Bruhn H, Hänicke W, Frahm J. Absolute concentrations of metabolites in the adult human brain *in vivo*: quantification of localized proton MR spectra. *Radiology* 1993; **187**: 219–227.
77. Blüml S, Seymour KL, Ross B. Developmental changes in choline- and ethanolimine-containing compounds measured with proton-decoupled 31P MRS in *in vivo* human brain. *Magn. Reson. Med.* 1999; **42**: 643–654.
78. Barker PB, Breiter SN, Soher BJ, Chathamn JC, Forder JR, Samphilipo MA, Magee CA, Anderson JA. Quantitative proton

spectroscopy of canine brain: *in vivo* and *in vitro* correlations. *Magn. Reson. Med.* 1994; **32**: 157–163.
79. Partington P, Feeney J, Burgen AS. The conformation of acetylcholine and related compounds in aqueous solution as studied by nuclear magnetic resonance spectroscopy. *Mol. Pharmacol.* 1972; **8**: 269–277.
80. Blüml S, Zuckerman E, Tan J, Ross BD. Proton-decoupled 31P magnetic resonance spectroscopy reveals osmotic and metabolic disturbances in human hepatic encephalopathy. *J. Neurochem.* 1998; **71**: 1564–1576.
81. Stoll AL, Renshaw PF, De Micheli E, Wurtman R, Pillay SS, Cohen BM. Choline ingestion increases the resonance of choline-containing compounds in human brain: an *in vivo* proton magnetic resonance study. *Biol. Psychiat.* 1995; **37**: 170–174.
82. Pfeuffer J, Tkác I, Provencher SW, Gruetter R. Toward an *in vivo* neurochemical profile: quantification of 18 metabolites in short-echo-time 1H NMR spectra of rat brain. *J. Magn. Reson.* 1999; **141**: 104–120.
83. Chang L, Ernst T, Osborn D, Seltzer W, Leonido-Yee M, Poland RE. Proton spectroscopy in myotonic dystrophy: correlations with CTG repeats. [See comments.] *Arch. Neurol.* 1998; **55**: 305–311.
84. Vermathen P, Govindaraju V, Matson GB, Maudsley AA. Detection of downfield 1H resonances in human brain using single voxel and SI methods. Proceedings of the International Society for Magnetic Resonance in Medicine, Abstract, p. 1584. (1999).
85. Ala-Korpela M, Posio P, Mattila S, Korhonen A, Williams SR. Absolute quantification of phospholipid metabolites in brain-tissue extracts by 1H NMR spectroscopy. *J. Magn. Reson. Ser. B* 1996; **113**: 184–189.
86. Lehmann A, Hagberg H, Jacobson I, Hamberger A. Effects of status epilepticus on extracellular amino acids in the hippocampus. *Brain Res.* 1985; **359**: 147–151.
87. Gruetter R, Ugurbil K, Seaquist ER. Steady-state cerebral glucose concentrations and transport in the human brain. *J. Neurochem.* 1998; **70**: 397–408.
88. Gyngell ML, Michaelis T, Hörstermann D, Bruhn H, Hänicke W, Merboldt KD, Frahm J. Cerebral glucose is detectable by localized proton NMR spectroscopy in normal rat brain *in vivo*. *Magn. Reson. Med.* 1991; **19**: 489–495.
89. Peres M, Bourgeois D, Roussel S, Lefur Y, Devoulon P, Remy C, Barrere B, Decorps M, Pinard E, Riche D, Benabid A-L, Seylaz J. Two-dimensional 1H spectroscopic imaging for evaluating the local metabolic response to focal ischemia in the conscious rat. *NMR Biomed.* 1992; **5**: 11–19.
90. Gruetter R, Garwood M, Ugurbil K, Seaquist ER. Observation of resolved glucose signals in 1H NMR spectra of the human brain at 4 Tesla. *Magn. Reson. Med.* 1996; **36**: 1–6.
91. Merboldt KD, Bruhn H, Hänicke W, Michaelis T, Frahm J. Decrease of glucose in the human visual cortex during photic stimulation. *Magn. Reson. Med.* 1992; **25**: 187–194.
92. Gruetter R, Novotny EJ, Boulware SD, Rothman DL, Shulman RG. 1H NMR studies of glucose transport in the human brain. *J. Cereb. Blood Flow Metab.* 1996; **16**: 427–438.
93. Gurst JE. NMR and the structure of deuterium-glucose. *J. Chem. Educ.* 1991; **68**: 1003–1004.
94. Perkins SJ, Johnson LN, Philips DC. High-resolution ^{1}H- and ^{13}C-N.M.R. spectra of D-glucopyranose, 2-acetamido-2-deoxy-D-glucopyranose, and related compounds in aqueous media. *Carbohydr. Res.* 1977; **59**: 19–34.
95. Koch HJ, Perlin AS. Synthesis and 13C N.M.R. spectrum of D-glucose-3-d. Bond polarization differences between the anomers of D-glucose. *Carbohydr. Res.* 1970; **15**: 403–410.
96. Curatolo W, Neuringer LJ, Ruben D, Haberkorn R. Two-dimensional *J*-resolved 1H-nuclear magnetic resonance spectroscopy of α,β-D-glucose at 500 MHz. *Carbohydr. Res.* 1983; **112**: 297–300.
97. Ross BD. Biochemical considerations in 1H spectroscopy. Glutamate and glutamine; *myo*-inositol and related metabolites. *NMR Biomed.* 1991; **4**: 59–63.
98. Westergaard N, Sonnewald U, Schousboe A. Metabolic trafficking between neurons and astrocytes: the glutamate/glutamine cycle revisited. *Devl. Neurosci.* 1995; **17**: 203–211.
99. Chamuleau RA, Bosman DK, Bovée WM, Luyten PR, den Hollander JA. What the clinician can learn from MR glutamine/glutamate assays. *NMR Biomed.* 1991; **4**: 103–108.
100. Pan JW, Mason GF, Pohost GM, Hetherington HP. Spectroscopic imaging of human brain glutamate by water-suppressed *J*-refocused coherence transfer at 4.1 T. *Magn. Reson. Med.* 1996; **36**: 7–12.
101. Thompson RB, Allen PS. A new multiple quantum filter design procedure for use on strongly coupled spin systems found *in vivo*: its application to glutamate. *Magn. Reson. Med.* 1998; **39**: 762–771.
102. Prost RW, Mark L, Mewissen M, Li SJ. Detection of glutamate/glutamine resonances by 1H magnetic resonance spectroscopy at 0.5 Tesla. *Magn. Reson. Med.* 1997; **37**: 615–618.
103. Kreis R, Farrow N, Ross BD. Localized 1H NMR spectroscopy in patients with chronic hepatic encephalopathy. Analysis of changes in cerebral glutamine, choline and inositols. *NMR Biomed.* 1991; **4**: 109–116.
104. Kanamori K, Ross BD. *In vivo* detection of N-15-coupled protons in rat brain by ISIS localization and multiple-quantum editing. *J. Magn. Reson.* 1999; **V139**:240–249.
105. Mason GF, Pan JW, Ponder SL, Twieg DB, Pohost GM, Hetherington HP. Detection of brain glutamate and glutamine in spectroscopic images at 4.1 T. *Magn. Reson. Med.* 1994; **32**: 142–145.
106. Gruetter R, Weisdorf SA, Rajanayagan V, Terpstra M, Merkle H, Truwit CL, Garwood M, Nyberg SL, Ugurbil K. Resolution improvements in *in vivo* 1H NMR spectra with increased magnetic field strength. *J Magn. Reson.* 1998; **135**: 260–264.
107. Meister A, Anderson ME. Glutathione. *A. Rev. Biochem.* 1983; **52**: 711–760.
108. Cooper AJ, Kristal BS. Multiple roles of glutathione in the central nervous system. *Biol. Chem.* 1997; **378**: 793–802.
109. Sian J, Dexter DT, Lees AJ, Daniel S, Agid Y, Javoy-Agid F, Jenner P, Marsden CD. Alterations in glutathione levels in Parkinson's disease and other neurodegenerative disorders affecting basal ganglia. [See comments.] *Ann. Neurol.* 1994; **36**: 348–355.
110. Brown FF, Campbell ID, Kuchel PW, Rabenstein DC. Human erythrocyte metabolism studies by 1H spin echo NMR. *FEBS Lett.* 1977; **82**: 12–16.
111. Mason RP, Cha GH, Gorrie GH, Babcock EE, Antich PP. Glutathione in whole blood: a novel determination using double quantum coherence transfer proton NMR spectroscopy. *FEBS Lett.* 1993; **318**: 30–34.
112. McKay CN, Brown DH, Reglinski J, Smith WE, Capell HA, Sturrock RD. Changes in glutathione in intact erythrocytes during incubation with penicillamine as detected by 1H spin-echo NMR spectroscopy. *Biochim. Biophys. Acta* 1986; **888**: 30–35.
113. Trabesinger AH, Weber OM, Duc CO, Boesiger P. Detection of glutathione in the human brain in vivo by means of double quantum coherence filtering. *Magn. Reson. Med.* 1999; **42**: 283–289.
114. Hillered L, Valtysson J, Enblad P, Persson L. Interstitial glycerol as a marker for membrane phospholipid degradation in the acutely injured human brain. *J. Neurol. Neurosurg. Psychiat.* 1998; **64**: 486–491.
115. Michaelis T, Helms G, Frahm J. Metabolic alterations in brain autopsies: proton NMR identification of free glycerol. *NMR Biomed.* 1996; **9**: 121–124.
116. Kinoshita Y, Kajiwara H, Yokota A, Koga Y. Proton magnetic resonance spectroscopy of brain tumors: an *in vitro* study. *Neurosurgery* 1994; **35**: 606–613. [Discussion 613–641].
117. Heindel W, Kugel H, Roth B. Noninvasive detection of increased glycine content by proton MR spectroscopy in the brains of two infants with nonketotic hyperglycinemia. *AJNR* 1993; **14**: 629–635.
118. Schwartz JC, Lampart C, Rose C. Histamine formation in rat brain *in vivo*: effects of histidine loads. *J. Neurochem.* 1972; **19**: 801–810.
119. Gadian DG, Proctor E, Williams SR, Cady EB, Gardiner RM. Neurometabolic effects of an inborn error of amino acid metabolism demonstrated *in vivo* by ^{1}H NMR. *Magn. Reson. Med.* 1986; **3**: 150–156.
120. Vermathen P, Capizzano A, Laxer KD, Matson GB, Maudsley AA. Enhancement of histidine detection *in vivo*. A new approach

for measuring brain pH. *Proceedings of the International Society for Magnetic Resonance in Medicine*, Abstract, 1999; p. 640.
121. Fogel WA, Andrzejewski W, Maslinski C. Neurotransmitters in hepatic encephalopathy. *Acta Neurobiol. Exp. (Warsz.)* 1990; **50**: 281–293.
122. Fogel WA, Andrzejewski W, Maslinski C. Brain histamine in rats with hepatic encephalopathy. *J. Neurochem.* 1991; **56**: 38–43.
123. Scriver CR. ed. The Metabolic and Molecular Bases of Inherited Disease, McGraw-Hill, New York 1995.
124. Vermathen P, Capizzano A, Maudsley AA. Administration and ^{1}H MRS detection of histidine in human brain: application to *in vivo* pH measurement. *Magn. Reson. Med.* 2000; **45**: 665–675.
125. Pisano JJ, Wilson JD, Cohen L, Abraham D, Udenfriend S. Isolation of gamma aminobutyrylhistidine (homocarnosine) from brain. *J. Biol. Chem.* 1961; **236**: 499–502.
126. Abraham D, Pisano JJ, Udenfriend S. The distribution of homocarnosine in mammals. *Arch. Biochem. Biophys.* 1962; **99**: 210–213.
127. Kish SJ, Perry TL, Hansen S. Regional distribution of homocarnosine, homocarnosine-carnosine synthetase and homocarnosinase in human brain. *J. Neurochem.* 1979; **32**: 1629–1636.
128. Perry TL, Kish SJ, Sjaastad O, Gjessing LR, Nesbakken R, Schrader H, Løken AC. Homocarnosinosis: increased content of homocarnosine and deficiency of homocarnosinase in brain. *J. Neurochem.* 1979; **32**: 1637–1640.
129. Perry TL, Hansen S, Gandham SS. Postmortem changes of amino compounds in human and rat brain. *J. Neurochem.* 1981; **36**: 406–410.
130. Gjessing LR, Lunde HA, Mrkrid L, Lenney JF, Sjaastad O. Inborn errors of carnosine and homocarnosine metabolism. *J. Neural Transm.* (Suppl.) 1990; **29**: 91–106.
131. Rothman DL, Behar KL, Prichard JW, Petroff OA. Homocarnosine and the measurement of neuronal pH in patients with epilepsy. *Magn. Reson. Med.* 1997; **38**: 924–929.
132. Dictionary of Organic Compounds, Chapman and Hall, New York 1982.
133. Brand A, Richter-Landsberg C, Leibfritz D. Multinuclear NMR studies on the energy metabolism of glial and neuronal cells. *Devl. Neurosci.* 1993; **15**: 289–298.
134. Shonk TK, Moats RA, Gifford P, Michaelis T, Mandigo JC, Izumi J, Ross BD. Probable Alzheimer disease: diagnosis with proton MR spectroscopy. *Radiology* 1995; **195**: 65–72.
135. Moats RA, Ernst T, Shonk TK, Ross BD. Abnormal cerebral metabolite concentrations in patients with probable Alzheimer disease. *Magn. Reson. Med.* 1994; **32**: 110–115.
136. Ross BD, Ernst T, Kreis R, Haseler LJ, Bayer S, Danielsen E, Blüml S, Shonk T, Mandigo JC, Caton W, Clark C, Jensen SW, Lehman NL, Arcinue E, Pudenz R, Shelden CH. 1H MRS in acute traumatic brain injury. *J. Magn. Reson. Imag.* 1998; **8**: 829–840.
137. Michaelis T, Helms G, Merboldt KD, Hänicke W, Bruhn H, Frahm J. Identification of *scyllo*-inositol in proton NMR spectra of human brain *in vivo*. *NMR Biomed.* 1993; **6**: 105–109.
138. Seaquist ER, Gruetter R. Identification of a high concentration of *scyllo*-inositol in the brain of a healthy human subject using 1H- and 13C-NMR. *Magn. Reson. Med.* 1998; **39**: 313–316.
139. Michaelis T, Frahm J. On the 3.35 ppm singlet resonance in proton NMR spectra of brain tissue: scyllo-inositol or methanol contamination? *Magn. Reson. Med.* 1995; **34**: 775–776.
140. Veech RL. The metabolism of lactate. *NMR Biomed.* 1991; **4**: 53–58.
141. Sappey-Marinier D, Calabrese G, Fein G, Hugg JW, Biggins C, Weiner MW. Effect of photic stimulation on human visual cortex, lactate and phosphates using 1H and 31P magnetic resonance spectroscopy. *J. Cereb. Blood Flow Metab.* 1992; **12**: 584–592.
142. Posse S, Dager SR, Richards TL, Yuan C, Ogg R, Artru AA, Müller-Gärtner HW, Hayes C. *In vivo* measurement of regional brain metabolic response to hyperventilation using magnetic resonance: proton echo planar spectroscopic imaging PEPSI. *Magn. Reson. Med.* 1997; **37**: 858–865.
143. Hurd RE, Freeman D. Proton editing and imaging of lactate. *NMR Biomed.* 1991; **4**: 73–80.
144. Novotny EJ, Avison MJ, Herschkowitz N, Petroff OA, Prichard JW, Seashore MR, Rothman DL. In vivo measurement of phenylalanine in human brain by proton nuclear magnetic resonance spectroscopy. *Pediatr. Res.* 1995; **37**: 244–249.
145. Stryer L. Biochemistry, W. H. Freeman, San Francisco, CA 1981.
146. Bick U, Ullrich K, Stöber U, Möller HE, Schuierer G, Ludolph AC, Oberwittler C, Weglage J, Wendel U. White matter abnormalities in patients with treated hyperphenylalaninaemia: magnetic resonance relaxometry and proton spectroscopy findings. *Eur. J. Pediatr.* 1993; **152**: 1012–1020.
147. Pietz J, Kreis R, Boesch C, Penzien J, Rating D, Herschkowitz N. The dynamics of brain concentrations of phenylalanine and its clinical significance in patients with phenylketonuria determined by *in vivo* 1H magnetic resonance spectroscopy. *Pediatr. Res.* 1995; **38**: 657–663.
148. Kreis R, Pietz J, Penzien J, Herschkowitz N, Boesch C. Identification and quantitation of phenylalanine in the brain of patients with phenylketonuria by means of localized *in vivo* 1H magnetic-resonance spectroscopy. *J. Magn. Reson. Ser. B* 1995; **107**: 242–251.
149. Möller HE, Vermathen P, Ullrich K, Weglage J, Koch HG, Peters PE. *In vivo* NMR spectroscopy in patients with phenylketonuria: changes of cerebral phenylalanine levels under dietary treatment. *Neuropediatrics* 1995; **26**: 199–202.
150. Pietz J, Kreis R, Schmidt H, Meyding-Lamadé UK, Rupp A, Boesch C. Phenylketonuria: findings at MR imaging and localized in vivo H-1 MR spectroscopy of the brain in patients with early treatment. *Radiology* 1996; **201**: 413–420.
151. Möller HE, Weglage J, Wiedermann D, Vermathen P, Bick U, Ullrich K. Kinetics of phenylalanine transport at the human blood–brain barrier investigated *in vivo*. *Brain Res.* 1997; **778**: 329–337.
152. Möller HE, Weglage J, Wiedermann D, Ullrich K. Blood–brain barrier phenylalanine transport and individual vulnerability in phenylketonuria. *J. Cereb. Blood Flow Metab.* 1998; **18**: 1184–1191.
153. Kohli A, Gupta RK, Poptani H, Roy R. In vivo proton magnetic resonance spectroscopy in a case of intracranial hydatid cyst. *Neurology* 1995; **45**: 562–564.
154. Hardy DL, Norwood TJ. Spectral editing techniques for the *in vitro* and *in vivo* detection of taurine. *J. Magn. Reson.* 1998; **133**: 70–78.
155. Roser W, Duc CO, Steinbrich W, Radue EW. Dangerous increase of taurine in the human brain after consumption of an 'energy drink'. *Proceedings of the International Society for Magnetic Resonance in Medicine*. Abstract, 1998 p. 1886.
156. Young SN. Behavioral effects of dietary neurotransmitter precursors: basic and clinical aspects. *Neurosci. Biobehav. Rev.* 1996; **20**: 313–323.
157. Haseler LJ, Sibbitt WJ, Sibbitt RR, Hart BL. Neurologic, MR imaging, and MR spectroscopic findings in eosinophilia myalgia syndrome. *AJNR* 1998; **19**: 1687–1694.
158. al Mardini H, Harrison EJ, Ince PG, Bartlett K, Record CO. Brain indoles in human hepatic encephalopathy. *Hepatology* 1993; **17**: 1033–1040.
159. Acworth IN, During MJ, Wurtman RJ. Processes that couple amino acid availability to neurotransmitter synthesis and release. In Amino Acid Availability and Brain Function in Health and Disease, G. Huether, Eds., pp. 117–136, Springer, Berlin (1987).
160. de Graaf RA, van Kranenburg A, Nicolay K. Off-resonance metabolite magnetization transfer measurements on rat brain in situ. *Magn. Reson. Med.* 1999; **41**: 1136–1144.
161. van Zijl PC, Barker PB. Magnetic resonance spectroscopy and spectroscopic imaging for the study of brain metabolism. *Ann. NY Acad. Sci.* 1997; **820**: 75–96.
162. Siegel GJ, Agranoff BW, Albers RW, Molinoff P. Basic Neurochemistry: Molecular, Cellular, and Medical Aspects, Raven Press, New York (1989).
163. Perry TL, Hansen S, Berry K, Mok C, Lesk D. Free amino acids and related compounds in biopsies of human brain. *J. Neurochem.* 1971; **18**: 521–528.

